


## RESEARCH ARTICLE

# Identification of atrial-enriched lncRNA *Walras* linked to cardiomyocyte cytoarchitecture and atrial fibrillation

Carlos García-Padilla<sup>1</sup> | Jorge N. Domínguez<sup>1</sup> | Valeria Lodde<sup>2,3</sup> | Rachel Munk<sup>2</sup> |  
 Kotb Abdelmohsen<sup>2</sup> | Myriam Gorospe<sup>2</sup> | Veronica Jiménez-Sábado<sup>4</sup> |  
 Antonino Ginel<sup>5,6</sup> | Leif Hove-Madsen<sup>4,6,7</sup> | Amelia E. Aránega<sup>1</sup> | Diego Franco<sup>1</sup> 

<sup>1</sup>Cardiovascular Development Group, Department of Experimental Biology, University of Jaen, Jaen, Spain

<sup>2</sup>Laboratory of Genetics and Genomics, National Institute on Aging IRP, National Institutes of Health, Baltimore, Maryland, USA

<sup>3</sup>Department of Biomedical Sciences, University of Sassari, Sassari, Italy

<sup>4</sup>CIBERCV, Barcelona, Spain

<sup>5</sup>Department Cardiac Surgery, Hospital de Sant Pau, Barcelona, Spain

<sup>6</sup>Biomedical Research Institute IIB Sant Pau, Barcelona, Spain

<sup>7</sup>Biomedical Research Institute Barcelona (IIBB-CSIC), Barcelona, Spain

## Correspondence

Diego Franco, Cardiovascular Development Research Group, Department of Experimental Biology B3-362, University of Jaen, 23071 Jaén, Spain.  
 Email: dfranco@ujaen.es

## Funding information

This work was supported by a grant-in-aid from the Junta de Andalucía Regional Council to DF and AA [CTS-446] and by a grant from the Ministry of Science, Innovation and Universities for the Spanish Government to AA and DF (BFU2015-67131P). VL, RM, KA, and MG were supported by the NIA IRP, NIH

## Abstract

Atrial fibrillation (AF) is the most prevalent cardiac arrhythmia in humans. Genetic and genomic analyses have recently demonstrated that the homeobox transcription factor Pitx2 plays a fundamental role regulating expression of distinct growth factors, microRNAs and ion channels leading to morphological and molecular alterations that promote the onset of AF. Here we address the plausible contribution of long non-coding (lnc)RNAs within the Pitx2>Wnt>miRNA signaling pathway. *In silico* analyses of annotated lncRNAs in the vicinity of the *Pitx2*, *Wnt8* and *Wnt11* chromosomal loci identified five novel lncRNAs with differential expression during cardiac development. Importantly, three of them, *Walaa*, *Walras*, and *Wallrd*, are evolutionarily conserved in humans and displayed preferential atrial expression during embryogenesis. In addition, *Walrad* displayed moderate expression during embryogenesis but was more abundant in the right atrium. *Walaa*, *Walras* and *Wallrd* were distinctly regulated by Pitx2, Wnt8, and Wnt11, and *Wallrd* was severely elevated in conditional atrium-specific Pitx2-deficient mice. Furthermore, pro-arrhythmogenic and pro-hypertrophic substrate administration to primary cardiomyocyte cell cultures consistently modulate expression of these lncRNAs, supporting distinct modulatory roles of the AF cardiovascular risk factors in the regulation of these lncRNAs. *Walras* affinity

**Abbreviations:** AF, atrial fibrillation; AngII, angiotensin II; ECG, electrocardiogram; GWAS, genome-wide association study; HTD, hyperthyroidism; HTN, hypertension; LC/MS/MS, liquid chromatography/mass spectrometry/mass spectrometry; lncRNA, long non coding RNA; MS, mass spectrometry; NE, norepinephrine.

This is an open access article under the terms of the Creative Commons Attribution-NonCommercial License, which permits use, distribution and reproduction in any medium, provided the original work is properly cited and is not used for commercial purposes.

© 2021 The Authors. *The FASEB Journal* published by Wiley Periodicals LLC on behalf of Federation of American Societies for Experimental Biology.

pull-down assays revealed its association with distinct cytoplasmic and nuclear proteins previously involved in cardiac pathophysiology, while loss-of-function assays further support a pivotal role of this lncRNA in cytoskeletal organization. We propose that lncRNAs *Walaa*, *Walras* and *Wallrd*, distinctly regulated by *Pitx2*>*Wnt*>*miRNA* signaling and pro-arrhythmogenic and pro-hypertrophic factors, are implicated in atrial arrhythmogenesis, and *Walras* additionally in cardiomyocyte cytoarchitecture.

#### KEYWORDS

atrial fibrillation, lncRNA, post-transcriptional regulation

## 1 | INTRODUCTION

Atrial fibrillation (AF) is the most common cardiac arrhythmia, with an incidence of 2%–3% in the general population that rises up to 8%–10% in the elderly. Genetic linkage analyses have identified point mutations in several ion channels with key roles in the configuration of the cardiac action potential, suggesting that they are implicated in AF. However, these genetic defects only explain a minority (<10%) of all AF cases. Seminal work by Gudbjartsson et al.<sup>1</sup> using genome-wide association studies (GWAS) revealed that risk variants in the 4q25 locus were highly associated to lone AF, postulating that regulatory elements within this locus might influence expression of a neighboring gene encoding the homeobox transcription factor *PITX2*, in turn leading to impaired cardiac function and AF. Subsequent GWAS studies and meta-GWAS analyses have increased exponentially our understanding of the plausible genetic substrates of AF, with the identification of more than 90 risk variants associated to AF.<sup>2</sup> Importantly, in all cases the most significant risk variants were those in the 4q25 locus. Experimental studies in mice have provided evidence that 4q25 physically interacts with the *Pitx2* promoter,<sup>3,4</sup> supporting key regulatory roles as suggested by Gudbjartsson et al.<sup>1</sup> In addition, systemic *Pitx2* loss-of-function experiments revealed increased susceptibility to atrial arrhythmias,<sup>5,6</sup> while conditional atrial-specific deletion of *Pitx2*, resulting in *Pitx2* insufficiency, led to spontaneous atrial arrhythmias.<sup>7</sup>

Subsequent studies demonstrated that *Pitx2* insufficiency led to remodeling of several meta-GWAS-associated genes, such as that encoding *Wnt8*, which in turn modulate *Wnt11* expression, leading to microRNA deregulation and hence impaired ion channels expression and function.<sup>7–9</sup> These data demonstrate a pivotal role of the *Pitx2*>*Wnt*>*microRNA* pathway modulating AF. In addition, experimentally induced AF leads to *Pitx2* downregulation, supporting the notion of a

self-perpetuating reduction of *Pitx2* during AF progression.<sup>10</sup> Moreover, cardiovascular risk factors contributing to increased frequency of AF onset in the human population, such as hypertension, hyperthyroidism and antioxidant redox imbalance, consistently altered the *Pitx2*>*Wnt*>*microRNA* pathway, underscoring a molecular link between these AF risk factors and specific cellular processes.<sup>11</sup>

The past two decades have revealed that gene regulatory networks are profoundly influenced by novel types of non-coding RNAs with regulatory potential. There is now extensive evidence that microRNAs are essential regulators of cardiovascular development and diseases, including seminal studies on the role of microRNAs regulating cardiac ion channels and AF itself. The discovery of long non-coding RNAs (lncRNAs) has increased the complexity of the non-coding RNA regulatory roles. lncRNAs generally have no protein-coding potential, yet many of them are structurally similar to mRNAs, including the presence of 5' terminal cap and 3' terminal poly(A) tails and their transcription by RNA polymerase II.<sup>12</sup> Similarly, most lncRNA genes comprise exons and introns and are often spliced. lncRNAs display lower expression levels and are more tissue-specific than protein-coding mRNAs,<sup>13</sup> supporting the notion that they may have tightly defined roles in different cellular events.<sup>14,15</sup> lncRNAs can be localized in both cytoplasm and nucleus; cytoplasmic lncRNAs are preferentially involved in post-transcriptional regulation while nuclear lncRNAs are predominantly involved in transcriptional regulation. Interestingly, lncRNAs can translocate from the nucleus to the cytoplasm and act therein.<sup>16</sup>

Distinct studies have investigated the functional role of cardiac-enriched lncRNAs during heart development, i.e., *Carmen*, *Braveheart*, and *Fendrr*. *Carmen*, miR-143 and miR-145 are located within the same genomic locus, but they are independently expressed.<sup>17,18</sup> Expression of *Carmen* in fetal and adult hearts is highly conserved in different mammalian species. Functionally, *Carmen* plays

a pivotal role at the earliest lineage commitment steps, modulating cardiac differentiation from initial mesoderm by regulating *Mesp1* expression.<sup>17</sup> Similarly, *Braveheart* is a key regulator in cardiac lineage commitment and its ablation leads to defective activation of key cardiac factors, heart development, and cardiomyocyte differentiation.<sup>19</sup> *Fendrr* is transiently expressed at the posterior end of the forming lateral plate mesoderm, and is required for the proper development of the heart and body walls.<sup>20,21</sup> We have recently demonstrated that these lncRNAs display a dynamic chamber-specific expression, are distinctly regulated by cardiac enriched transcription factors such as *Mef2c*, *Srf* and *Nkx2.5* and display distinct isoform usage during cardiogenesis.<sup>22</sup>

In the context of AF, several reports have provided evidence of altered expression of certain lncRNAs<sup>23–26</sup> but scarce information is available about their tissue distribution and regulatory mechanisms. Gore-Panter et al.<sup>27</sup> identified *PANCR* as an intergenic lncRNA expressed in the adult left atrium from a region adjacent to *PITX2*, and is expressed in coordination with *PITX2C* mRNA during cardiomyocyte differentiation. Importantly, *PANCR* is expressed in human tissues but no orthologues have been found in other species.<sup>27</sup>

In this study, we have investigated the expression of lncRNAs via processes regulated by *Pitx2>Wnt>miRNA*. *In silico* analyses of annotated lncRNAs expressed from the vicinity of *Pitx2*, *Wnt8* and *Wnt11* chromosomal loci identified five novel lncRNAs showing differential expression levels during cardiac development in mice and some of them are also evolutionarily conserved in humans. Three of them displayed preferential atrial-specific expression during embryogenesis and were distinctly regulated by *Pitx2*, *Wnt8* and *Wnt11* as well as by microRNAs such as *miR-1*, *miR-133* and *miR-29*. Furthermore, pro-arrhythmogenic and pro-hypertrophic substrates such as angiotensin II, norepinephrine and thyroid hormone administration distinctly regulate their expression. *Walras* pulldown and loss-of-function assays further demonstrate a key role of this lncRNA in cardiomyocyte cytoskeletal organization. In summary, we have identified novel lncRNAs with enhanced atrial expression that are distinctly regulated by signaling pathways leading to atrial arrhythmogenesis.

## 2 | MATERIALS AND METHODS

### 2.1 | Mouse breeding and tissue sampling

CD1 mice were bred and embryos were collected at different embryonic developmental stages, ranging from

embryonic day (E) E12.5 to E18.5. Neonatal (1 day old) and adult (>6 months) hearts were also collected. Pregnant females, adult and neonatal mice were euthanized by cervical dislocation. Neonates were previously placed on ice. Subsequently, embryonic and postnatal hearts were dissected into right atrium, left atrium and ventricular chambers, pooled and stored in liquid nitrogen until used. Additionally, distinct tissues such as spleen, liver, lungs, small and large intestine, kidney and brain were also dissected from adult mice, pooled and stored in liquid nitrogen until used.

The *Pitx2*<sup>flxed</sup> and *NppaCre* transgenic mouse lines and the generation of conditional atrial (*NppaCre*) mutant mice were previously described.<sup>7,8,28,29</sup> Two different conditions were used for the *NppaCrePitx2* mice: wild-type Cre controls (*NppaCre*<sup>-</sup>*Pitx2*<sup>fl/fl</sup>) and atrial-specific homozygous (*NppaCre*<sup>+</sup>*Pitx2*<sup>-/-</sup>). This investigation conforms with the Guide for the Care and Use of Laboratory Animals published by the US National Institutes of Health. The study was approved by the University of Jaén Bioethics Committee.

### 2.2 | Mouse genotyping and phenotyping

DNA for PCR screening was extracted from adult ear and/or tail samples. Screening of Cre and *Pitx2* floxed alleles was routinely done using specific primers as previously described.<sup>7</sup> Cycling conditions for *Cre* DNA were as follows: 5 min at 95°C, 35 cycles of 30 s at 95°C, 30 s at 60°C and 90 s at 72°C: and for *Pitx2* DNA as follows: 5 min at 95°C, 40 cycles of 30 s at 95°C, 30 s at 60°C and 90 s at 72°C, followed by a final extension step of 10 min at 72°C. In addition, the expression levels of *Pitx2* mRNA in left atrial samples of wild-type Cre controls (*NppaCre*<sup>+</sup>*Pitx2*<sup>fl/fl</sup>) and atrial-specific homozygous (*NppaCre*<sup>+</sup>*Pitx2*<sup>-/-</sup>) were assessed by RT-qPCR analysis, displaying in all cases 60%–70% reduction in *PITX2c* expression in *NppaCre*<sup>+</sup>*Pitx2*<sup>-/-</sup> samples.

### 2.3 | Mouse tissue samples

Genetically modified transgenic *Pitx2* mice and their corresponding controls were sacrificed by cervical dislocation. Adult hearts were carefully dissected and briefly rinsed in Ringer's solution. Left atrium tissue samples were collected for each experimental condition, immediately snap-frozen in liquid nitrogen, and stored at –80°C until used. Pooled samples of at least three independent mice were processed for each condition, respectively. Three independent pooled samples were further processed for RNA isolation and RT-qPCR analysis.

## 2.4 | Human atrial biopsies

Atrial myocardial tissue samples were obtained from patients undergoing cardiac surgery at Hospital de la Santa Creu i Sant Pau (Barcelona). Specimens were obtained from the right atria just prior to atrial cannulation for cardiopulmonary bypass. After excision, samples were rapidly frozen in liquid nitrogen and stored at  $-80^{\circ}\text{C}$  until analyzed. The atrial samples were classified as patients with (AF;  $n = 4$ ) and without (No AF;  $n = 3$ ) a recorded history of AF. Clinical data are presented in Table S1. Although the atrial tissue samples consisted of tissue that would normally be discarded during surgery, permission to be used in this study was obtained from each patient. The study was approved by the Ethical Committee of the Hospital de la Santa Creu i Sant Pau (Barcelona) and the investigation conforms with the principles outlined in the Declaration of Helsinki.

## 2.5 | RNA isolation and cDNA synthesis

Total RNA was isolated using Trizol (Roche) according to manufacturer's guidelines and DNase treated using RNase-Free DNase (Roche) for 1 h at  $30^{\circ}\text{C}$ . In all cases, at least three distinct pooled samples were used to perform the corresponding RT-qPCR experiments.

First strand cDNA was synthesized at  $50^{\circ}\text{C}$  for 1 h using  $1\ \mu\text{g}$  of RNA, oligo-dT primers and Superscript III Reverse Transcriptase (Invitrogen) according to manufacturer's guidelines. Negative controls to assess genomic contamination were performed for each sample, without reverse transcriptase, which resulted in all cases in no detectable amplification product.

## 2.6 | qPCR analyses (mRNA and lncRNA)

RT-PCR was performed in Mx3005Tm QPCR System with an MxPro QPCR Software 3.00 (Stratagene) and SyBR Green detection system. Reactions were performed in 96-well plates with optical sealing tape (Cultek) in  $20\ \mu\text{l}$  total volume containing SYBR Green Mix (Finnzymes) and the corresponding cDNA. Two internal controls, mouse *Gusb* and *Gapdh* mRNAs, were used in parallel for each run and represented as previously described.<sup>8,9</sup> Amplification conditions were as follows: denaturalization step of  $95^{\circ}\text{C}$  for 10 min, followed by 40 cycles of  $95^{\circ}\text{C}$  for 30 s,  $60^{\circ}\text{C}$  for 30 s,  $72^{\circ}\text{C}$  for 30 s; with final elongation step of  $72^{\circ}\text{C}$  for 10 min. All primers were designed to span exon-exon boundaries using online Primer3 software Primer3input (<http://bioinfo.ut.ee/primer3-0.4.0/>). Primer sequences

are provided in Table S2. No amplifications were observed in PCR control reactions containing only water as the template. Each PCR reaction was performed at least three times to obtain representative averages. The Livak method was used to analyze the relative quantification RT-PCR data<sup>30</sup> and normalized in all cases taking as 100% the wild-type (control) value, as previously described.<sup>7</sup>

## 2.7 | qPCR analyses (microRNA)

microRNA RT-qPCR was performed using Exiqon LNA microRNA reverse transcription (RT) followed by real-time quantitative (q) PCR primers and detection kit according to the manufacturer's guidelines. All reactions were always run in triplicate using 5S as normalizing control, as recommended by the manufacturer. SyBR Green was used as quantification system on a Stratagene Q-Max 2005P RT-qPCR thermocycler. Relative measurements were calculated as described by Livak and Schmittgen<sup>30</sup> and control measurements were normalized to represent 100% as previously described.<sup>7</sup>

## 2.8 | Plasmid, siRNA, microRNA mimics cell transfections

HL1 cells ( $6 \times 10^5$  cells per well) were transfected with plasmids containing expression constructs for *Pitx2c*, *Wnt8a* (Addgene), *Wnt11a* (Addgene, Cambridge, MA, USA) and with pre-miR-1, pre-miR-133, pre-miR-29 (Exiqon) or siRNA-*Pitx2c*, siRNA-*Wnt8a*, siRNA-*Wnt11a*, siRNA-*Gm44934/Walras* (Sigma, Aldrich, Munich, Germany), respectively, as previously described.<sup>6,7</sup> siRNA sequences are provided in Table S3.

## 2.9 | Immunofluorescence analyses

Control and experimentally siRNA treated cells were collected after the corresponding treatment, rinsed in PBS for 10 min at room temperature, and fixed with 1% PFA for 2 h at  $4^{\circ}\text{C}$ . After fixation, the samples were rinsed three times (10 min each) in PBS at room temperature and then permeabilized with 1% Triton X-100 in PBS for 30 min at room temperature. To block nonspecific binding sites, PBS containing 5% goat serum and 1% bovine serum albumin (Sigma) was applied to the cell cultures overnight at  $4^{\circ}\text{C}$ . Phalloidin-Atto 488 (Sigma) was used, diluted (5 mg/ml) in PBS, and applied to each culture overnight at  $4^{\circ}\text{C}$ . Subsequently, the samples were rinsed three times (for 1 h each) in PBS to remove excess Phalloidin-Atto 488. Finally, they were incubated with DAPI (1:1000; Sigma) for 7 min

at room temperature and rinsed three times in PBS for 5 min each. Alternatively to Phalloidin-Atto 488 staining, control and experimentally siRNA treated cells were immunofluorescently labelled to detect ACTN1, ACTN4 and MYH9 expression, respectively. Primary antibodies against ACTN1 (ab68194), ACTN4 (ab108198), MYH9 (ab75590) were used, diluted (1:200) in PBS, and applied to each culture overnight at 4°C, respectively. Subsequently, the samples were rinsed three times (for 1 h each) in PBS to remove excess primary antibody and incubated 2 hours at room temperature with Alexa-Fluor 546, 488 and 633 anti-rabbit (1:100; Invitrogen) as secondary antibody. Cell cultures were stored in PBS in darkness at 4°C until analysed using a Leica TCS SP5 II confocal scanning laser microscope.

## 2.10 | Cell culture and angiotensin II, norepinephrine and thyroid hormone treatment

Primary cultures of mouse fetal (E17.5) cardiomyocytes were isolated using standard procedures,<sup>31</sup> cultured accordingly and treated with 1 µM angiotensin II (AngII), 100 µM norepinephrine (NE) and 10 nM thyroid T3/T4 hormone, respectively, as previously reported.<sup>9,32,33</sup>

## 2.11 | Nuclear/cytoplasmic distribution

Cytoplasmic and nuclear RNA fractions from atrial and ventricles samples were isolated with Cytoplasmic & Nuclear RNA Purification Kit (Norgen, Belmont, CA, USA) following the manufacturer's instructions. After RNA isolation, RT-qPCR analysis for nuclear enriched *Rpb1* mRNA marker and cytoplasmic *Gapdh* mRNA marker were performed to validate enrichment on each subcellular fractions. RT-qPCR analysis of distinct lncRNAs was subsequently performed as detailed above.

## 2.12 | lncRNA pull down assays

Biotinylated RNA of exon 1 and exon2 of Gm\_44934 of Exon 1 and Exon 2 were synthesized from PCR fragment using specific forward primers that contained the T7 RNA polymerase promoter sequence [(T7), CCAAGCTTCTAATACGACTCACTATAGGGAGA]. After purifying the DNA template, biotinylated transcripts were synthesized using MaxiScript T7 kit (Ambion); whole-cell lysates (500 µg) from HL1 cells were incubated with 1 µg of biotinylated RNA for 2 h at room temperature. Complexes were isolated with Streptavidin-coupled Dynabeads (Invitrogen) and analyzed by MS.

For MS analysis, peptide mixtures from each sample were loaded onto a peptide trap cartridge and eluted onto a reversed-phase PicoFrit column (New Objective, Woburn, MA, USA). Eluted peptides were ionized and sprayed into the mass spectrometer, using a Nanospray Flex Ion Source ES071 (Thermo Scientific). The LC/MS/MS analysis of samples were carried out using a Thermo Scientific Q-Exactive hybrid Quadrupole-Orbitrap Mass Spectrometer and a Thermo Dionex UltiMate 3000 RSLCnano System. Proteins were identified using the Thermo Proteome Discoverer 1.4.1 platform. Database search against public mouse protein database from NCBI was performed through the Proteome Discoverer 1.4.1 platform.

## 2.13 | miRNA pull down assays

Biotinylated miR-29 was synthesized by IDT technologies. Whole-cell lysates (500 µg) from HL1 cells were incubated with 1 µg of biotinylated RNA for 2 h at room temperature. Complexes were isolated with Streptavidin-coupled Dynabeads (Invitrogen) following the protocol published by Panda et al.<sup>34</sup> RNA associated to biotinylated miR-29 was isolated using *Direct-zol™ RNA Miniprep Plus* (Zymo research) following the manufacturer's instructions and RT-qPCR was subsequently performed as detailed above. Biotinylated miR-23 was used as a negative control.

## 2.14 | RIP assay

For immunoprecipitation of endogenous ACTN1, ACTN4 and MYH9 cytoskeleton proteins, HL1 cells were lysed with PEB buffer for 10 min on ice and centrifuged at 10 000 g for 15 min at 4°C. The supernatants were incubated with protein A Sepharose beads (Abcam) coated with antibodies that recognized ACTN1, ACTN4, MYH9 or control IgG (Abcam) for 2 h at 4°C, respectively. The corresponding beads were washed with NT2 buffer (50 mM Tris-HCl [pH 7.5], 150 mM NaCl, 1 mM MgCl<sub>2</sub>, 0.05% NP-40). Protein complexes were incubated with 20 units of DNase I (15 min at 37°C). In this step, an aliquot from each reaction was isolated for Western blot validation. Subsequently they were further incubated with 0.1% SDS/0.5 mg/ml Proteinase K (30 min at 55°C) to remove DNA and proteins, respectively. The RNA isolated from the IP materials were further assessed by RT-qPCR analysis.

## 2.15 | Western blot

For western blot analysis, 10% of total IP lysate was used. Primary antibodies recognizing ACTN1 (ab68194),

ACTN4 (ab108198), MYH9 (ab75590) from Abcam were used. After incubation with the rabbit secondary antibodies, protein signals were developed using HRP.

## 2.16 | Statistical analyses

For statistical analyses of datasets, unpaired Student's *t*-tests were used. Significance levels or *p* values are stated in each corresponding figure legend. *p* < .05 was considered statistically significant.

## 3 | RESULTS

### 3.1 | Identification of novel lncRNAs putatively involved in the Pitx2>Wnt>microRNA pathway

Previous studies have demonstrated that some long non coding RNAs act locally regulating neighboring genes.<sup>35–38</sup> We therefore examined the mouse genome to identify lncRNAs in close vicinity to genes previously identified to play a pivotal role in the onset of AF, particularly Pitx2>Wnt>microRNA pathway.<sup>7–9</sup> In particular, we searched for lncRNAs expressed from regions close to the *Pitx2*, *Wnt8* and *Wnt11* loci. We did not find novel lncRNAs near the *Pitx2* locus, besides the previously reported *Playrr* lncRNA,<sup>39</sup> but we identified two lncRNAs adjacent to *Wnt8* and four near *Wnt11* genes, respectively (Figure 1A; Table 1). Three of them, i.e., *Walras*, *Wallrd* and *Walce* are evolutionarily conserved in humans (Figure S1). In particular, *Walras* displayed significant homology, ranging from 25% to 43%, with three distinct human lncRNAs (AP0002340.1, AP000785.1 and LINC02761). *Wallrd* isoforms also displayed significant homology, ranging from 33% to 45%, with AC13382.1, AC13382.2 and AC104116.1, respectively. Finally, *Walce* display significant homology (35%) with *Wnt11\_03* human lncRNA (Figure S1).

We then measured the levels of expression of these lncRNAs in the right and left atria and in ventricular tissues of mouse embryos ranging from E12.5 to E18.5, neonate and adult tissues. Among the six lncRNAs interrogated, including *Playrr*, only five of them were detectable in cardiac tissues (Figure 1B–F). Three of them (*Walaa*, *Walras* and *Wallrd*) displayed a preferential embryonic expression confined to the atrial chambers with only low ventricular expression. Interestingly, *Walaa* displayed a similar atrial-specific expression in both right and left atrial chambers, peaking at E16.5 (Figure 1B), *Walras* displayed a left atrial-restricted expression (Figure 1D), with peak levels at E16.5, while *Wallrd* also displayed atrial-restricted expression, preferentially in the left atrium, at

E16.5 (Figure 1F). In all cases, expression in neonatal and adult heart was markedly lower than in embryonic heart. Importantly, *Walrad* displayed preferential expression in the right atrium in all stages analyzed (Figure 1C), including adulthood, but also presented a transient peak expression at neonatal stages in the ventricular chambers. By contrast, *Walce* was preferentially expressed in embryos but was not restricted to the atrial chambers (Figure 1E), showing a dynamic expression pattern in right atrium, left atrium and ventricular tissues at different developmental time points. *Playrr* displayed a prominent expression in the early developmental stages declining during development (Figure 1G). Curiously, expression of these lncRNAs is significantly different from the expression of *Wnt8* and *Wnt11* mRNAs expression during cardiogenesis, as illustrated in Figure 1H–I. Expression of these five distinct lncRNAs is not restricted to the heart, since all but *Walce* are also expressed in distinct adult tissues such as spleen, liver, lungs, gut, kidney and brain as depicted in Figure 2A–F. *Walce* expression is restricted to the heart and spleen (Figure 2D). Importantly, *Wnt8* mRNA is also broadly expressed in distinct adult tissues (Figure 2H), while *Wnt11* mRNA is primarily expressed in the heart and brain, with low, but detectable levels in spleen and lungs (Figure 2G). In summary, we identified novel lncRNAs with wide distribution in adult tissues and importantly, three of them, *Walaa*, *Walras* and *Wallrd*, display preferential expression in the embryonic atrial chambers and one of them, *Walrad*, with preferential expression in the adult right atrium during cardiogenesis. Furthermore, their expression profile, both in different adult tissues as well as during cardiogenesis, is markedly distinct from those of *Wnt8* and *Wnt11* mRNAs, supporting the notion that they might not directly regulate Wnt expression.

### 3.2 | Differential spatio-temporal nuclear vs cytoplasmic localization of these novel lncRNAs support both transcriptional and post-transcriptional regulatory function

lncRNAs can reside in both the nucleus and the cytoplasm, exerting distinct regulatory functions in each compartment. We thus measured the relative abundance of these lncRNAs in the nucleus and cytoplasm by RT-qPCR analysis using *Rpb1* mRNA for normalization<sup>22</sup> (Figure S2). The nuclear and cytoplasmic distribution was analyzed in three distinct cardiac compartments of E14.5 mouse embryos and neonatal mice: right atrium, left atrium and ventricles. *Walas* displayed similar nuclear vs cytoplasmic distribution in the left atrium in both embryonic and adult stages, while it was prominently nuclear in the embryonic and adult ventricles. Importantly, a rise in cytoplasmic levels of

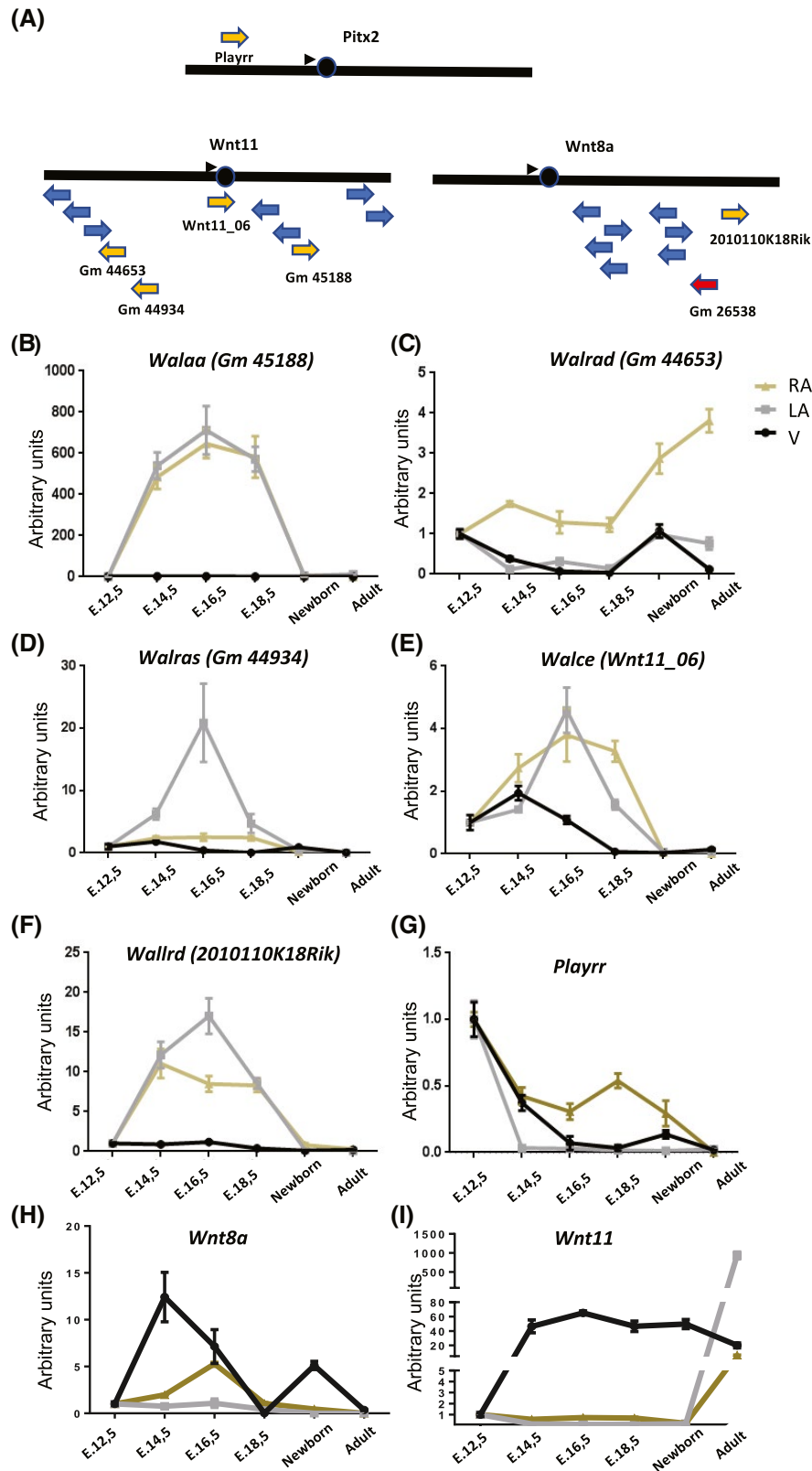


**FIGURE 1** (A) Schematic representation of the mouse chromosomal localization of lncRNAs situated in the vicinity of *Pitx2*, *Wnt11* and *Wnt8a* genes. (B–G) RT-qPCR analyses of *Walaa*, *Walras*, *Wallrd*, *Walrad*, *Walce* and *Playrr* expression levels. We note observe atrial expression of *Walaa*, *Walras* and *Wallrd* during cardiogenesis, while *Walrad* is mainly expressed in the left atrium in the adulthood. (H–I) RT-qPCR analyses of *Wnt11* and *Wnt8a* expression during cardiogenesis. Three embryonic hearts were pooled on each developmental time and three distinct neonatal and adult hearts were used for RNA isolation, respectively. Three independent biological assays were analyzed in each case

TABLE 1 Transcripts and gene localization data of novel identified lncRNAs

LncRNA name (new)	LncRNA name (previous)	Transcript number	Type	Chromosome position	Isoforms	Bps
Walras	Gm 44934	ENSMUST00000208941.1	LncRNA	Chromosome 7: 98,734,747-98,735,081 reverse strand	1	238
Walaa	Gm 45188	ENSMUST00000207592.1	LncRNA	Chromosome 7: 98,895,930-98,899,545 forward strand	1	1369
Walrad	Gm 44653	ENSMUST00000208543.1	LncRNA	Chromosome 7: 98,720,057-98,728,760 reverse strand	1	4610
Walce	Wnt11_06	ENSMUST00000208062.1	LncRNA	Chromosome 7: 98,835,112-98,855,195 forward strand.	1	745
Wallrd	2010110K18Rik	ENSMUST00000181453.2	LncRNA	Chromosome 18: 34,751,809-34,758,685 forward strand	3	2398
		ENSMUST00000181641.1				678
		ENSMUST00000236940.1				490

*Walras* was observed from embryonic to neonatal stages in the right atrium (Figure 3A). *Walrad* was prominently nuclear in both embryonic and neonatal stages in the left and right atria, while similar nuclear/cytoplasmic distribution was observed in the embryonic and neonatal ventricles (Figure 3B). *Walras* displayed no significant differences in the left atrium at both stages analyzed, while in the right atrium and ventricle it was prominently nuclear in the embryonic stages whereas there were no significant differences in the neonatal stage (Figure 3C). *Walce* displayed a prominent nuclear distribution in the left atrium at both stages, but no significant differences in the right atrium and ventricles (Figure 3D). *Wallrd* displayed similar nuclear and cytoplasmic expression levels in the embryonic and adult left atrium and ventricles. Importantly, however, *Wallrd* shifted from being primarily cytoplasmic in the embryonic right atrium to being mostly nuclear in the adult ventricles (Figure 3E). Finally, *Playrr* displays similar nuclear vs cytoplasmic distribution at all tissues and stages analyzed except in the embryonic left atrium where it is prominently nuclear (Figure 3F). Overall, these data demonstrate distinct spatio-temporal and subcellular distribution for these lncRNAs, suggesting chamber-specific shifts in their transcriptional vs post-transcriptional regulatory roles during cardiac development.

### 3.3 | LncRNA regulatory roles exerted by Pitx2, Wnt8 and Wnt11

To dissect the functional roles of Pitx2, Wnt8 and Wnt11 in the regulation of these newly identified lncRNAs, overexpression and silencing experiments were carried out in atrial HL1 cardiomyocytes.

*Pitx2c* overexpression and silencing significantly upregulated *Walaa*, *Walrad* and *Walce*, downregulates *Wallrd* while *Walras* display no significant differences

(Figure 4A). *Wnt8a* overexpression significantly decreased all lncRNAs analyzed except *Wallrd*. *Wnt8a* siRNA silencing significantly decreased *Walaa* and *Walras*, upregulated *Walce* while *Walrad* and *Wallrd* displayed no significant differences (Figure 4B). On the other hand, *Wnt11* overexpression significantly upregulated all lncRNAs analyzed except *Walaa*, which was downregulated. Importantly, silencing *Wnt11* using small interfering (si)RNA also upregulated all lncRNAs analyzed except *Walras* (Figure 4C). Control experiment of gain- and loss-of-function are provided in Figure 4A–C (right). These data indicate that *Pitx2*, *Wnt8a* and *Wnt11* influenced the expression levels of these lncRNAs. Moreover, *Pitx2* silencing upregulated *Walrad* and *Walce*, while *Wnt8* and *Wnt11* overexpression displayed complementary patterns on the regulation of *Walrad* and *Walce* expression, in line with our previous findings in *NppaCrePitx2<sup>-/-</sup>* mice.<sup>7</sup> In addition, it is importantly to note that both *Pitx2* overexpression and silencing similarly affected lncRNAs, demonstrating that even subtle changes in *Pitx2* expression greatly influenced lncRNA abundance, although the precise regulatory molecular mechanisms remain to be elucidated.

To further support the notion that *Pitx2* regulates the expression of these lncRNAs, we measured lncRNA levels of these lncRNAs in conditional *Pitx2* mouse model *NppaCrePitx2<sup>-/-</sup>*. Left atrial samples were used to verify *Pitx2* loss-of-function by measuring *Pitx2c* mRNA levels using RT-qPCR analysis (Figure 4D). As previously reported, *NppaCrePitx2<sup>-/-</sup>* mice displayed 70%–80% reduction of *Pitx2c* mRNA expression levels in the left atrial chamber (Figure 4D, right), leading to *Pitx2* insufficiency. In this context, *Walaa* was severely upregulated, *Wallrd* moderately upregulated, while *Walrad* was downregulated, and *Walras* and *Walce* displayed no significant differences in abundance (Figure 4D). These data support our earlier observations in HL1 cardiomyocytes that *Pitx2* regulates *Walaa* but not *Walras*. The surprising finding that *Walrad*

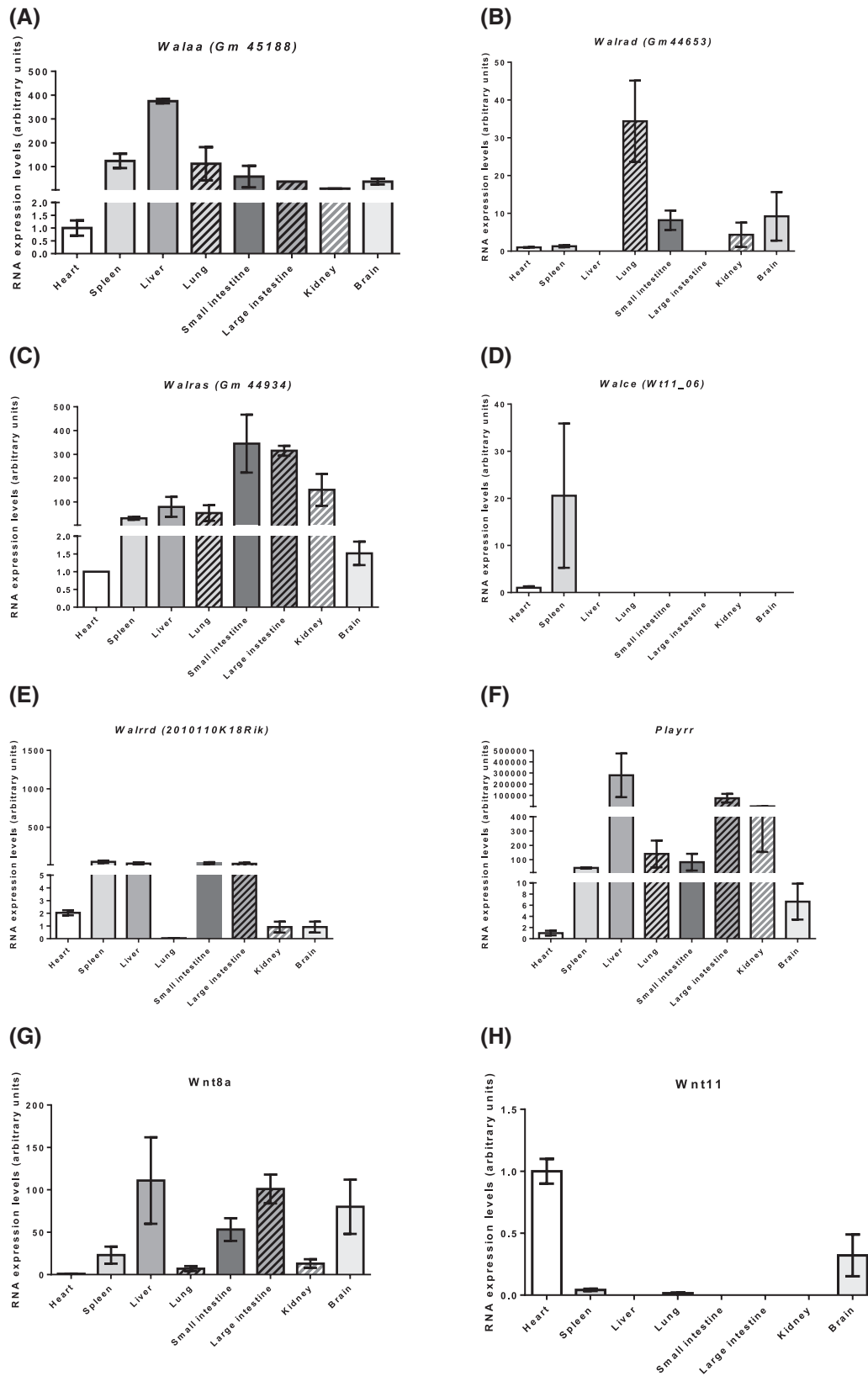


**FIGURE 2** (A–H) RT-qPCR analyses of *Walaa*, *Walras*, *Walrrd*, *Walrad*, *Walce*, *Playrr*, *Wnt8a*, and *Wnt11* expression levels in different organs (heart, spleen, liver, lung, small intestine, large intestine, kidney, and brain) in the adult mouse. Note that *Walaa*, *Walras*, *Walrrd*, *Walrad*, *Playrr*, and *Wnt8a* are widely distributed in different organs, while *Walce* is essentially confined to the spleen and heart, and *Wnt11* to the heart and brain with just detectable levels in the spleen and lungs. Three independent adult tissues were used for RNA isolation, respectively. Three independent biological assays were analyzed in each case

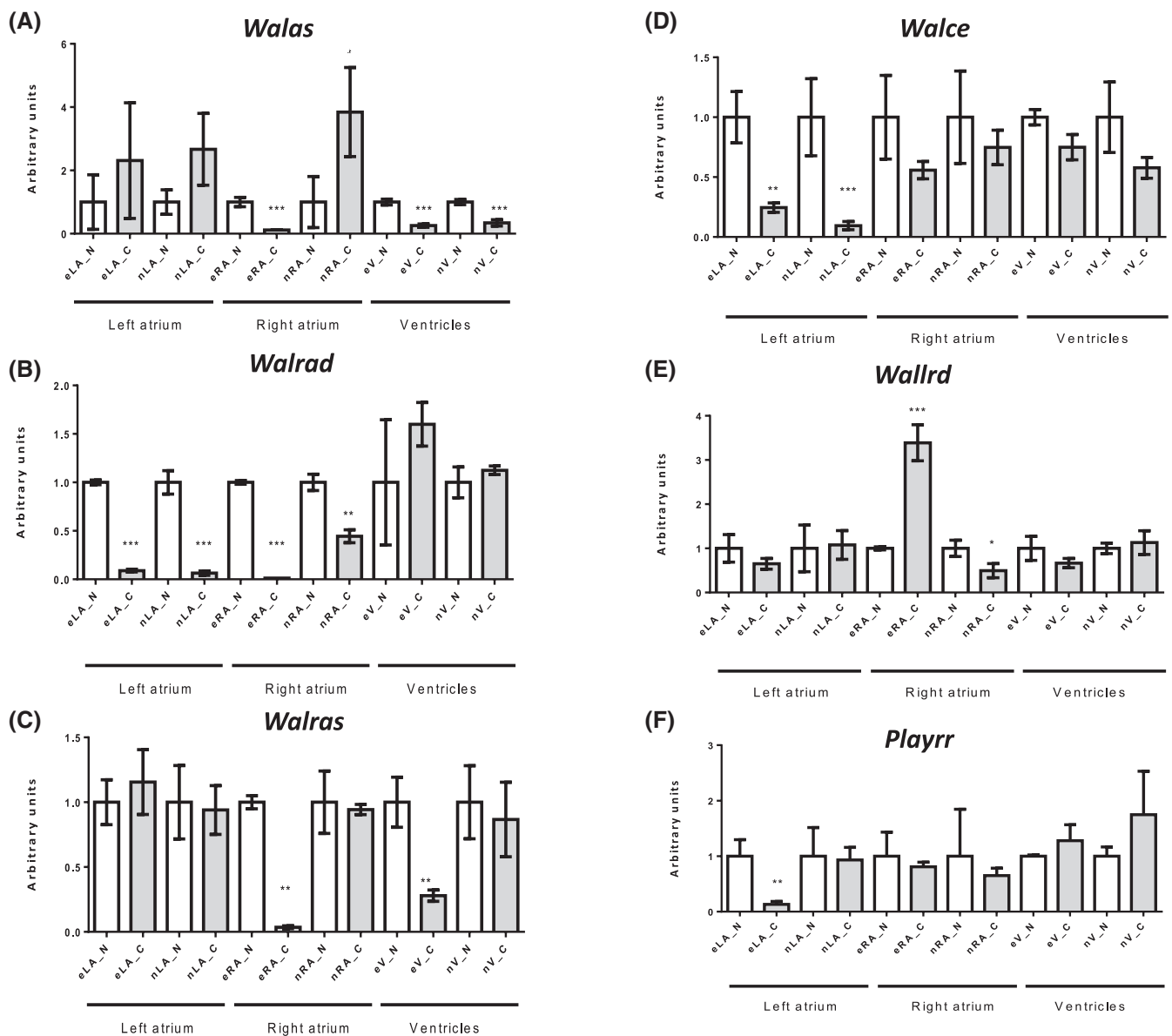
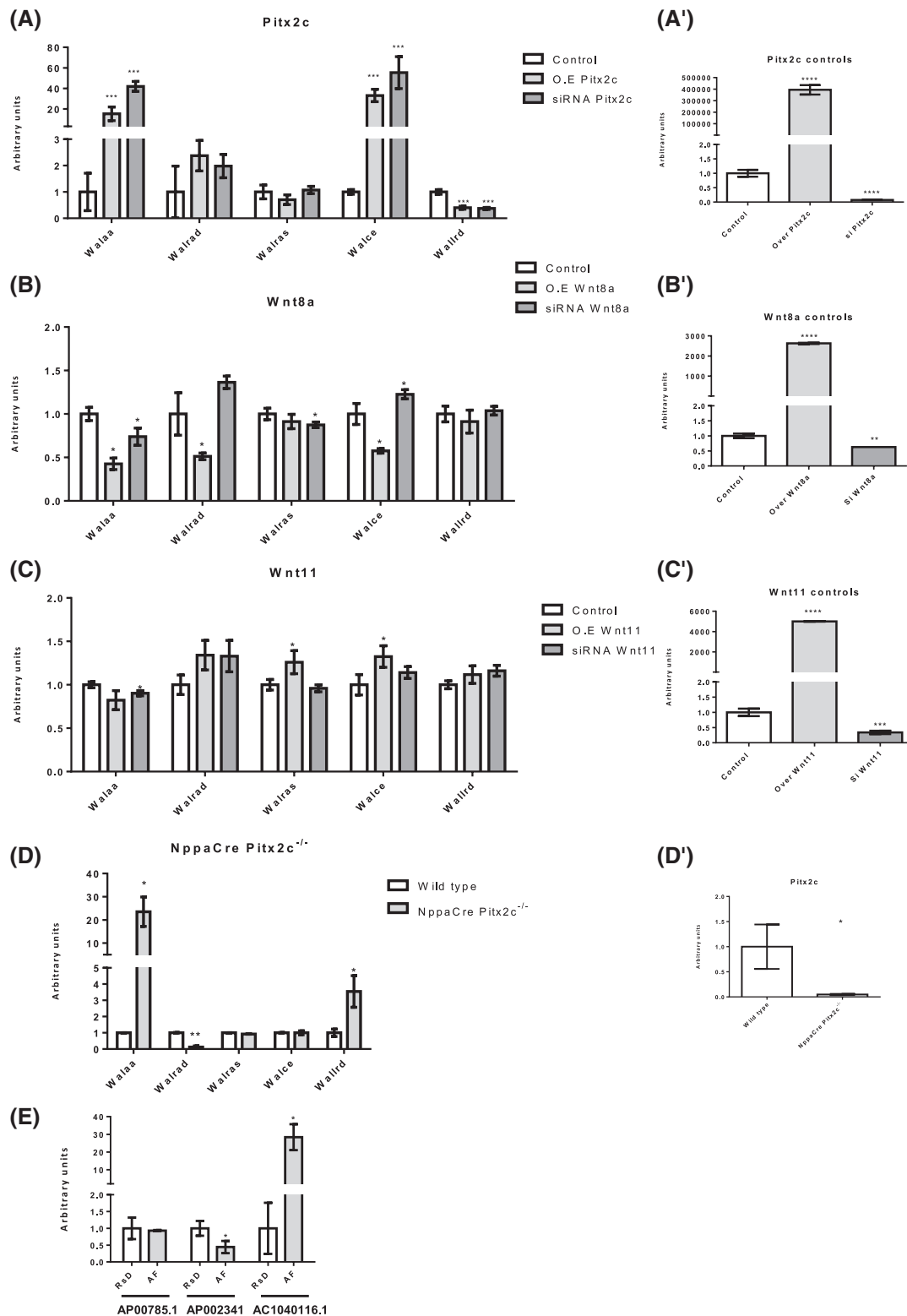


**FIGURE 3** (A–F) Nuclear vs cytoplasmic distribution of *Walas*, *Walrad*, *Walras*, *Walce*, *Wallrd* and *Playrr* in the embryonic and neonatal right atrium, left atrium and ventricles, respectively. Differential nuclear vs cytoplasmic subcellular distribution was observed for *Walas*, *Walras* and *Wallrd* in the right atrium of both embryonic and neonatal hearts, while *Walras* only displayed it in the embryonic right atrium. *Walas* displayed enhanced nuclear localization in the embryonic and neonatal ventricles while *Walras* only did in the embryonic ventricle. *Walrad* and *Walce* displayed enhanced nuclear vs cytoplasmic localization in embryonic and neonatal left atrium. Five to ten embryonic right atrial, left atrial or ventricles were pooled on each developmental staged, respectively and used for RNA isolation. Three independent biological assays were performed on each case. Statistical analyses was performed using unpaired Student's *t*-test. \* $p < .05$ , \*\* $p < .01$ , \*\*\* $p < .005$ . eLA\_N, embryonic left atrium, nuclear, eLA\_C, embryonic left atrium, cytoplasmic, eRA\_N, embryonic right atrium, nuclear, eRA\_C, embryonic right atrium, cytoplasmic, eV\_N, embryonic ventricle, nuclear, eV\_C, embryonic ventricle, cytoplasmic, nLA\_N, neonatal left atrium, nuclear, nLA\_C, embryonic left atrium, cytoplasmic, nRA\_N, neonatal right atrium, nuclear, nRA\_C, neonatal right atrium, cytoplasmic, nV\_N, neonatal ventricle, nuclear, nV\_C, neonatal ventricle, cytoplasmic

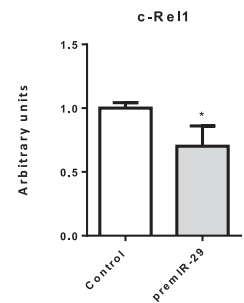
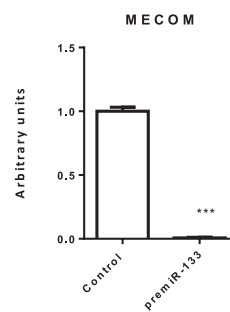
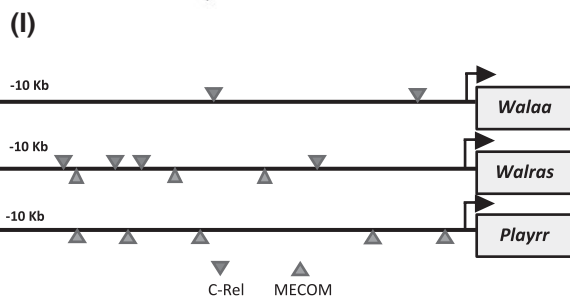
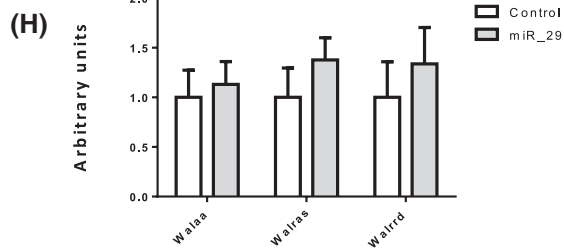
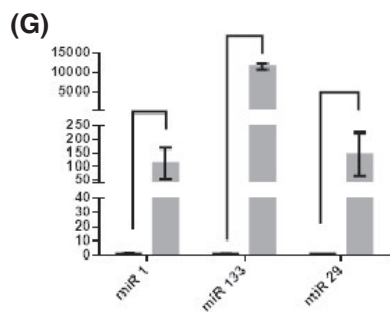
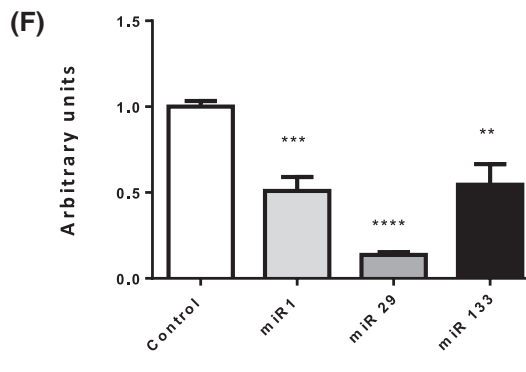
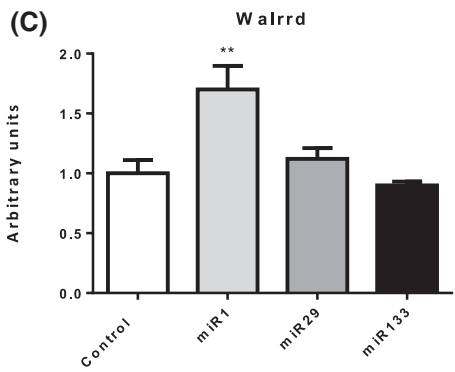
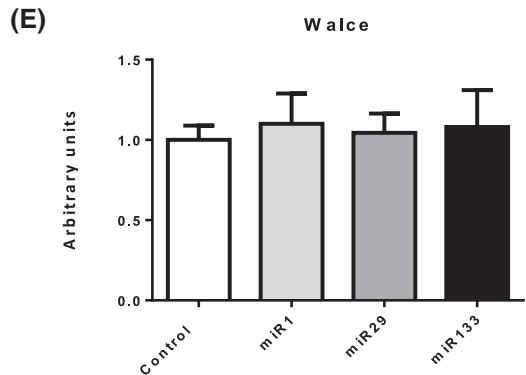
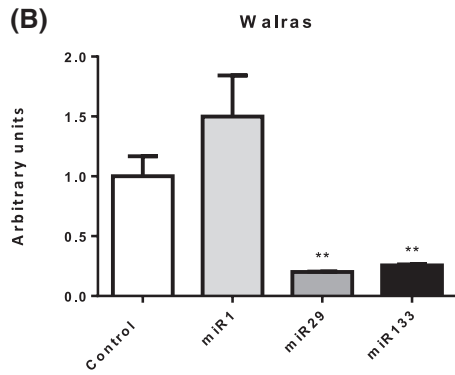
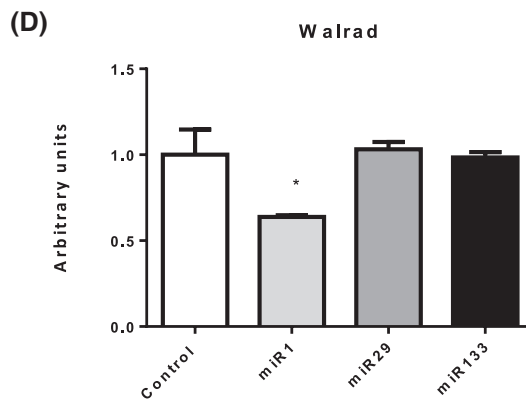
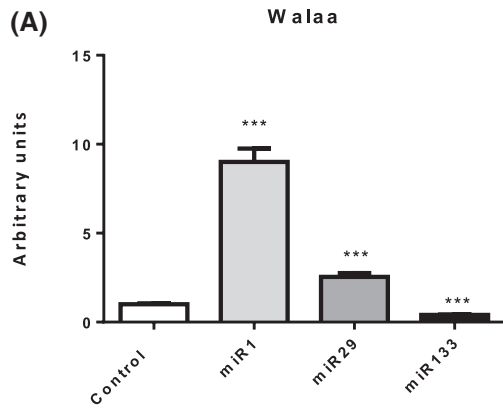
and *Wallrd* display opposite patterns in *NppaCrePitx2*<sup>-/-</sup> mice and HL1 Pitx2 siRNA assays demonstrate that additional studies are required to clarify this point.

Since we identified plausible human lncRNAs homologues for *Walras*, *Wallrd* and *Walce*, we also investigated if these conserved lncRNAs are deregulated in AF patients. Right atrial biopsies of AF and no AF patients

were subsequently scrutinized. Our data demonstrate that AP00785.1 displayed no significant differences while AP002340.1 is significantly decreased while AC1040116.1 was significantly increased in AF as compared to no AF patients (Figure 4E). The other identified human homologues displayed no detectable expression (data not shown). Therefore these data further confirmed the upregulation



**FIGURE 4** (A–C) *Right*, RT-qPCR analyses of the levels of *Walaa*, *Walrad*, *Walras*, *Walce* and *Wallrd* after overexpression or silencing of *Pitx2*, *Wnt8* and *Wnt11*, respectively. *Left*, levels of *Pitx2*, *Wnt8* and *Wnt11* mRNAs after overexpression and silencing. (D) *Right*, Expression levels of *Walaa*, *Walras* and *Wallrd* in *NppaCrePITX2<sup>-/-</sup>* adult left atrial chambers; *Left*, *Pitx2c* mRNA levels in *NppaCrePITX2<sup>-/-</sup>* adult left atrial chambers. (E) Expression levels of AP00785.1, AP002341 (*Walras* human homologue) and AC1040116.1 (*Wallrd* human homologue) in human right atrial biopsies of patients with sinus rhythm (RsD) (i.e., no AF) and atrial fibrillation (AF), respectively. Three independent siRNA and overexpression assays were analyzed in each case. Similarly, at least three independent biopsies corresponding to each condition were analyzed in each case. Statistical analyses were performed using unpaired Student's *t*-test. \**p* < .05, \*\**p* < .01, \*\*\**p* < .005, \*\*\*\**p* < .001





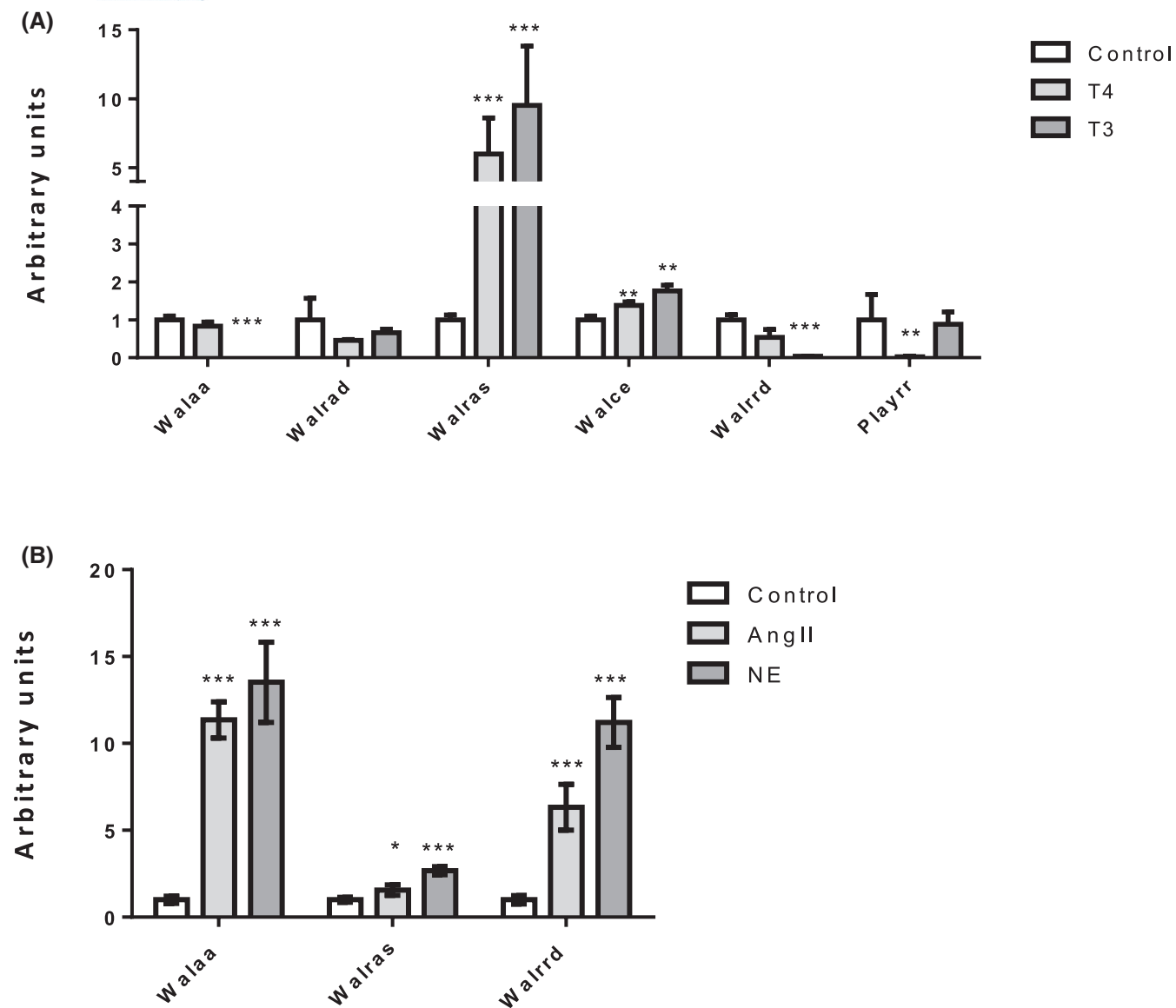


**FIGURE 6** (A) RT-qPCR analyses of the levels of *Walaa*, *Walrad*, *Walras*, *Walce*, *Wallrd*, and *Playrr* after T3 or T4 thyroid hormone administration in HL1 atrial cardiomyocytes, respectively. T3 administration significantly suppressed *Walaa* and *Wallrd* levels and increased *Walras* and *Walce* levels while T4 administration increased *Walras* and *Walce* but downregulated *Playrr* while no changes are observed for *Walaa*, *Walrad* and *Wallrd*. (B) RT-qPCR analyses of the levels of *Walaa*, *Walras*, and *Wallrd* after angiotensin II (AngII) or norepinephrine (NE) administration. Both, AngII and NE treatments enhances *Walaa*, *Walras* and *Wallrd* expression. Three independent assays were analyzed in each case. Statistical analyses were performed using unpaired Student's *t*-test. \* $p < .05$ , \*\*\* $p < .005$ , \*\*\*\* $p < .001$

and NE, respectively, as previously reported,<sup>8</sup> and lncRNA expression was assessed by RT-qPCR analysis. Our data indicate that AngII and NE administration, respectively, significantly enhanced the levels of *Walaa*, *Wallrd* and *Walras* (Figure 6B). In line with our previous findings after thyroid hormone administration, these data therefore support a plausible role of these lncRNAs in AF pathophysiology.

### 3.7 | *Walras* lncRNA pull down assays

To examine more deeply the function of the atrium-specific *Walras* lncRNA, we sought to identify the

proteins interacting with it. To this end, we prepared lysates from HL1 cells and biotinylated *Walras*. After incubation, lncRNA-protein complexes were pulled down and the associated proteins were identified by LC-MS/MS. A total of 40 proteins significantly interacting with *Walras* were identified (Table 2). Among them, ~40% were cytoplasmic proteins, 12% were nuclear and 20% mitochondrial, supporting a function dual role for *Walras* in the nucleus and cytoplasm, in line with our nuclear/cytoplasmic distribution analyses (Figure 3C). Among the cytoplasmic proteins, *Walras* associated with three distinct myosin proteins, MYH6, MYH9 and MYH10; interestingly, MYH6 is a structural protein that forms part of

TABLE 2 Identification of *Walrus* interacting proteins as revealed by pull-down assays followed by LC-MS/MS analyses

Accessiona	UniprotKB-ID	Gene	Short-name	Subcellular location	Gene ontology (roles)
71152969	Q61879	MYH10	Myosin-10	Cytoplasm, cell projection, lamellipodium	Actin cytoskeleton organization
205371802	Q8VDD5	MYH9	Myosin-9	Cytoplasm, cytoskeleton	Actin cytoskeleton reorganization
3024204	Q02566	MYH6	Myosin-6	Cytoplasm, myofibril. Note=Thick filaments of the myofibrils	Actin filament-based movement
146345422	P06745	G6PI	Glucose-6-phosphate isomerase	Cytoplasm. Secreted	Angiogenesis
146345481	P09411	PGK1	Phosphoglycerate kinase 1	Cytoplasm	Glycolytic process
13123946	P57780	ACTN4	Alpha-actinin-4	Cytoplasm	Actin filament bundle assembly
341940814	Q9D379	HYEP	Epoxide hydrolase 1	Microsome membrane; Single-pass type II membrane protein. ER membrane	Aromatic compound catabolic process
224471907	Q9WTP6	KAD2	Adenylate kinase 2, mitochondrial	Mitochondrion intermembrane space	ADP biosynthetic process
124028629	O88569	ROA2	Heterogeneous nuclear ribonucleoproteins A2/B1	Nucleus, nucleoplasm. Cytoplasm	mRNA processing
46397834	P51150	RAB7A	Ras-related protein Rab-7a	Cytoplasm vesicle, phagosome membrane	Bone resorption
48429104	P61979	HNRPK	Heterogeneous nuclear ribonucleoprotein K	Cytoplasm	mRNA processing
115718	P18242	CATD	Cathepsin D	Lysosome. Melanosome	Autophagosome assembly
353526354	P17751	TPIS	Triosephosphate isomerase	Mitochondrion matrix	Gluconeogenesis
60390645	Q9DCN2	NB5R3	NADH-cytochrome b5 reductase	Isoform 1: ER membrane	Cholesterol biosynthetic process
46395721	Q7TPR4	ACTN1	Alpha-actinin-1	Cytoplasm, cytoskeleton	Actin crosslink formation
20178035	Q9DBJ1	PGAM1	Phosphoglycerate mutase 1	Mitochondrion matrix	Glycolytic process
338817898	P05201	AATC	Aspartate aminotransferase, cytoplasmic	Cytoplasm	2-oxoglutarate metabolic process
267190	Q02053	UBA1	Ubiquitin-like modifier-activating enzyme 1	Cytoplasm	Cellular response to DNA damage stimulus
94730421	Q99P72	RTN4	Reticulon-4	ER membrane	Axonal fasciculation
5915871	O35887	CALU	Calumenin	ER lumen. Melanosome	Peripheral nervous system axon regeneration
52000730	Q921G7	ETFD	Electron transfer flavoprotein-ubiquinone oxidoreductase, mitochondrial	Mitochondrion inner membrane	Electron transport chain
124964	P09055	ITB1	Integrin beta-1	Cell membrane	Axon extension
1350822	P49312	ROA1	Heterogeneous nuclear ribonucleoprotein B	Nucleus. Cytoplasm. Shuttles continuously between the nucleus and the cytoplasm	Alternative mRNA splicing, via spliceosome
549057	P80315	TCPD	T-complex protein 1 subunit delta	Cytoplasm. Melanosome	Binding of sperm to zona pellucida
266608	Q01768	NDKB	Nucleoside diphosphate kinase B	Cytoplasm. Cell membrane. Cell projection, lamellipodium	Activation of mitophagy in response to mitochondrial depolarization
118542	P26443	DHE3	Glutamate dehydrogenase 1, mitochondrial	Mitochondrion matrix	Glutamate biosynthetic process

(Continues)

TABLE 2 (Continued)

Accessiona	UniprotKB-ID	Gene	Short-name	Subcellular location	Gene ontology (roles)
81896595	Q8BLF1	NCEH1	Neutral cholesterol ester hydrolase 1	Membrane	Lipid catabolic process
29839593	Q91W90	TXND5	Thioredoxin domain-containing protein 5	ER lumen	Apoptotic cell clearance
118105	P17742	PPIA	Peptidyl-prolyl cis-trans isomerase A	Cytoplasm. Secreted	Lipid particle organization
61217662	Q9ZIN5	DX39B	Spliceosome RNA helicase Ddx39b	Nucleus	Cellular response to DNA damage stimulus
50400807	O35114	SCRB2	Lysosome membrane protein 2	Lysosome membrane	Cell adhesion
6093768	Q60930	VDAC2	Voltage-dependent anion-selective channel protein 2	Mitochondrion outer membrane	Negative regulation of intrinsic apoptotic signalling pathway
46577116	Q9D1G1	RAB1B	Ras-related protein Rab-1B	Cytoplasm	Autophagy
71153826	Q7TPV4	MBB1A	Myb-binding protein 1A	Nucleus	Cellular response to glucose starvation
1709998	P53994	RAB2A	Ras-related protein Rab-2A	ER-Golgi intermediate compartment membrane; Lipid-anchor. Melanosome	Golgi organization
342187049	P26039	TLN1	Talin-1	Cell projection, ruffle membrane	Cell-substrate junction assembly
341940396	P52825	CPT2	Carnitine O-palmitoyltransferase 2, mitochondrial	Mitochondrion inner membrane	Fatty acid metabolic process
66773808	Q9JH15	IVD	Isovaleryl-CoA dehydrogenase, mitochondrial	Mitochondrion matrix	Fatty acid beta-oxidation using acyl-CoA dehydrogenase
51702234	P62897	CYC	Cytochrome c, somatic	Mitochondrion intermembrane space. Loosely associated with the inner	Apoptotic process
51701449	Q9CQA3	SDHB	Succinate dehydrogenase [ubiquinone], iron-sulfur subunit, mitochondrial	Mitochondrion inner membrane	Respiratory electron transport chain

Note: Observed that 40 interacting proteins were identified, most of them are located in the cytoplasm, with a small but significant fraction is also observed in other cellular organelles such as the nucleus, mitochondria and endoplasmic reticulum.

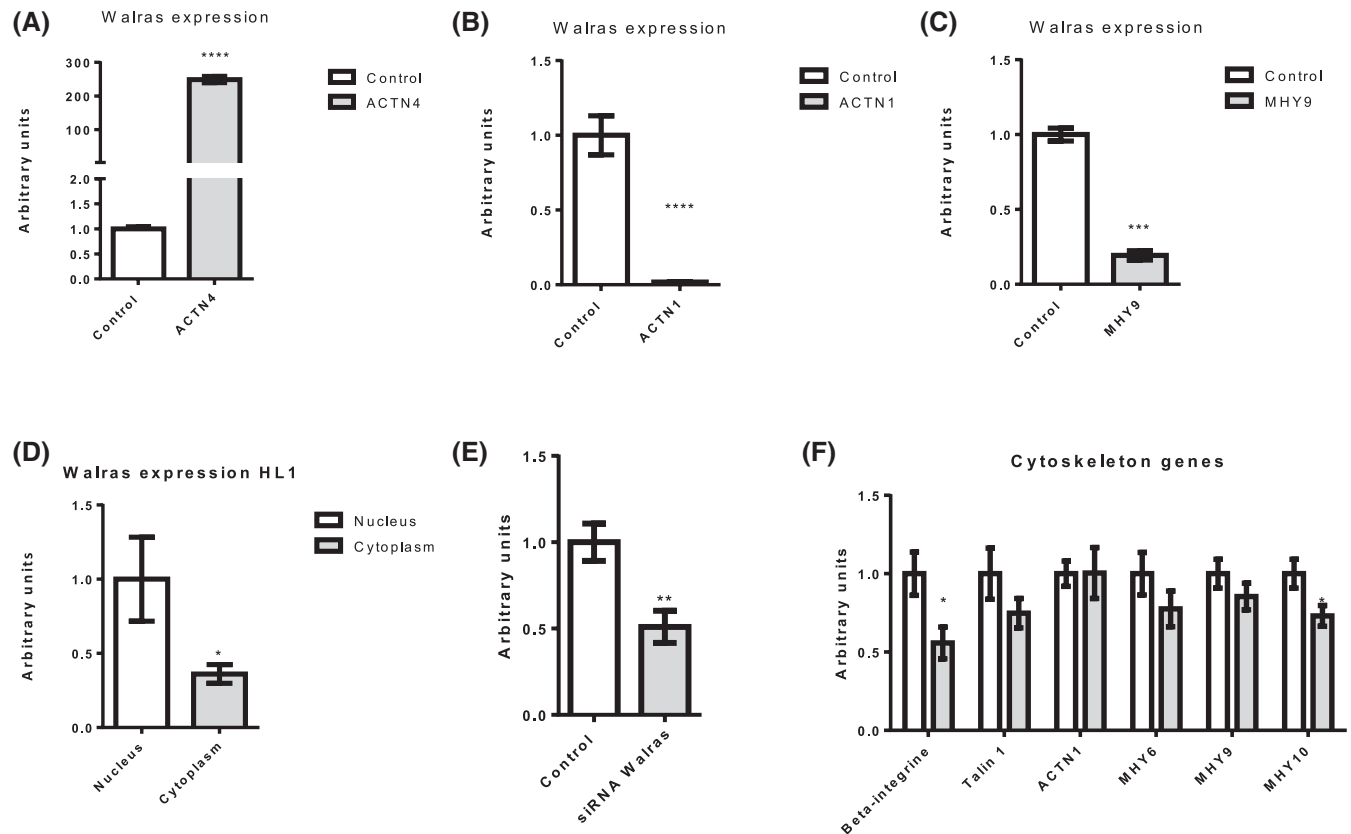


**FIGURE 7** (A–C) RIP assays for ACTN4 (A), ACTN1 (B) and MHY9 (C), respectively. (D) RT-qPCR analyses of *Walras* nuclear and cytoplasmic distribution in HL1 atrial cardiomyocytes. (E) *Walras* levels 24 h after siRNA transfection. (F) RT-qPCR analyses of genes encoding for *Walras* interacting proteins in cells transfected with *Walras* siRNA (grey bars) as compared to controls (white bars)

the sarcomere and is frequently altered in cardiac pathological conditions such as cardiac hypertrophy<sup>45–47</sup> as well as more recently with AF.<sup>48</sup> Several cytoskeletal proteins RAB1A, RAB2A, RAB7A, ACTN1, ACTN4, TLN1 and ITB1 are also associated to *Walras*. Importantly several of these proteins are linked to WNT non-canonical signaling pathway and at least one of them (ACTN4) has been recently linked to AF.<sup>49</sup> Among the nuclear proteins, *Walras* was found to interact with ROA2, ROA1, DXC39B and MBBIA, suggesting that it can also play a nuclear role, possibly in transcription, although at present the functions of these interacting proteins are poorly understood. Surprisingly, *Walras* also interacted with a large array of mitochondrial proteins, such as KAD2, ETFD, DHE3, VDAC2, IVD, CYC and SDHB, as well as with proteins located in other subcellular organelles, particularly at the ER (RTN-4, CALU, TXDN5); the functional consequences of these interactions remain to be explored. In sum, these data revealed the complexity of *Walras*-interacting proteins and pave the ways for dissecting the functional role of this lncRNA in a cardiovascular context. Validation of the *Walras* pulldown assays were performed for a subset of these interacting proteins (Figure 7A–C). We demonstrated by RIP assays in HL1 cardiomyocytes that ACTN4,

but not ACTN1 and MHY9, directly interact with *Walras* (Figure 7A–C). Importantly, *Walras* is distributed in both, nuclear and cytoplasmic compartments in HL1 cardiomyocytes (Figure 7D), in line with our observations in embryonic and neonatal cardiac chambers (Figure 3C). Further support of *Walras* lncRNA-protein interactions is provided as qPCR analyses of distinct *Walras* interacting proteins failed to display differential expression in siRNA *Walras* treated cells at mRNA level, except for integrin beta 1 (*Itb1*).

To further support the plausible functional role of *Walras* in cardiomyocytes, we designed siRNAs and performed loss-of-function assays in HL1 cardiomyocytes. RT-qPCR analyses demonstrated significant knock-down of *Walras* in HL1 cardiomyocytes (Figure 7E). Immunohistochemical analyses in HL1 cardiomyocytes demonstrated that cells treated with *Walras* siRNAs display significantly decreased cell-cell interactions (Figure 8B,C) as compared to controls (Figure 8A,C) and cytoskeletal rearrangements (Figure 8A–C). Immunocytochemical assays of ACTN4 (Figure 8D–F), ACTN1 (Figure 8G–I) and MHY9 (Figure 8J–L) distribution evidenced a significant downregulation of these cytoskeletal proteins in *Walras* siRNA treated HL1 cardiomyocytes.

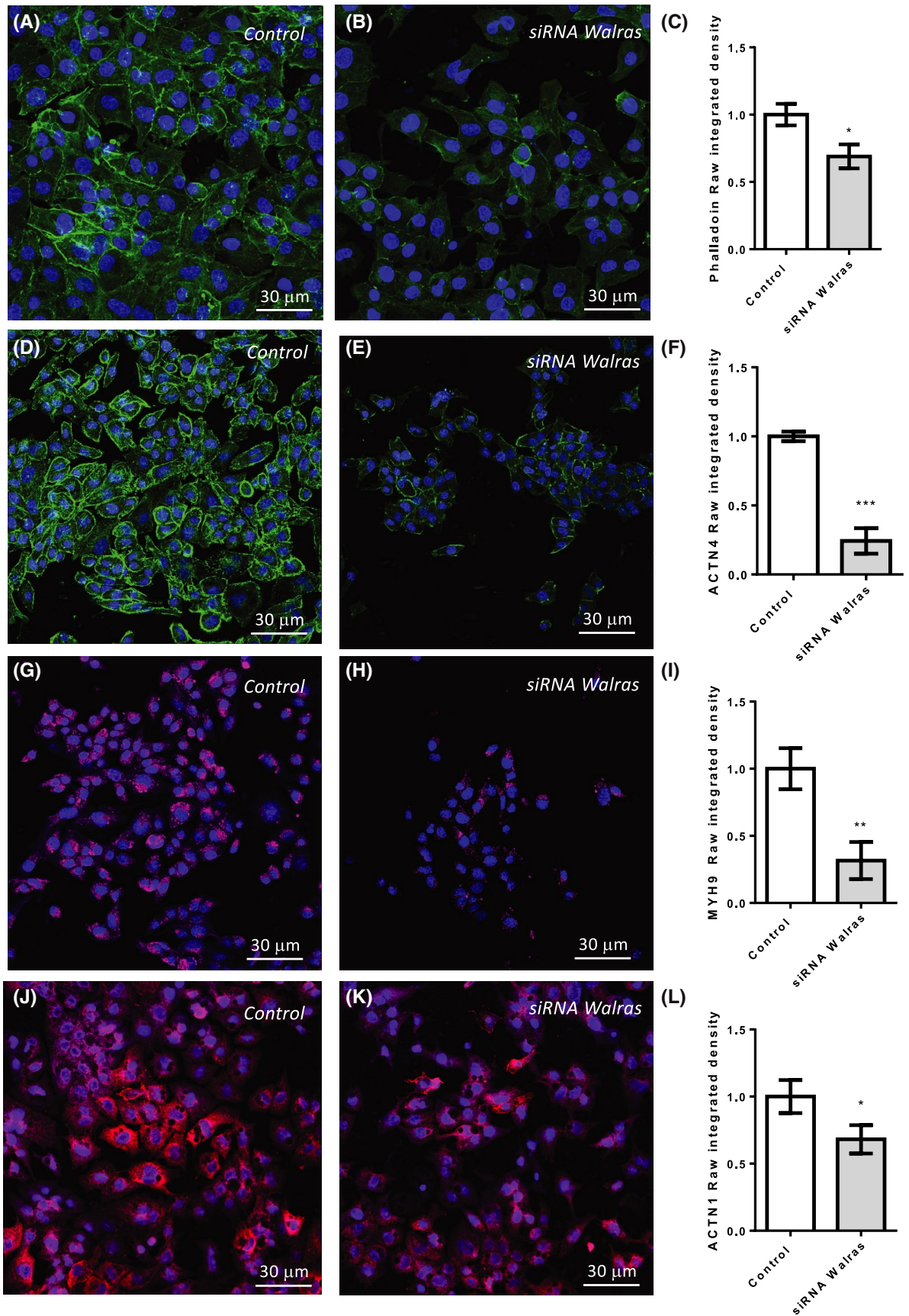


**FIGURE 8** Immunohistochemical analyses of control (A,D,G,J) and *Walras* silenced (B,D,H,K) cardiomyocytes stained with phalloidin (A,B), anti-ACTN4 (D,E), anti-ACTN1 (G–H) and MYH9 (J–K). Note that cell-cell interactions are disrupted in all *Walras* siRNA conditions, and that phalloidin (C), ACTN4 (F), ACTN1 (I) and MYH9 (L) stainings are significantly decreased. DAPI staining (blue) identify cell nuclei

## 4 | DISCUSSION

AF is the most common cardiac arrhythmia in humans, with an estimated incidence of 2%–4% in the general population, but rising up to 8%–10% in the elderly. Mechanistically, AF is initiated by impaired electrical activity that is most frequently originated in the left atrium, particularly in the vicinity of the entrance of pulmonary veins. The onset of AF leads to structural and electrical remodeling of both the left and right atrial chambers leading to self-perpetuation.<sup>50</sup>

Over the past few decades, our understanding of the genetic basis of AF has increased greatly. A large number of studies provided evidence on the causal relationship between distinct point mutations in multiple genes encoding ion channels and the occurrence of AF. More recently, a seminal paper by Gudbjartsson et al.<sup>1</sup> identified risk variants at 4q25 highly associated to lone AF and subsequently corroborated in distinct AF cohort studies.<sup>51–55</sup> These variants are located 150 kb downstream of the homeobox transcription factor PITX2. Importantly, loss-of-function assays in mice showed that impaired Pitx2 function leads to increased atrial arrhythmia susceptibility.<sup>5–7</sup> Wang et al.<sup>5</sup> demonstrated aberrant embryonic *Shox2* and *Tbx3* expression in Pitx2 loss-of-function and related such impaired expression to AF susceptibility. Kirchhof et al.<sup>6</sup> reported similar findings and demonstrated that the expression of multiple ion channels was impaired. Importantly, in both cases, no AF episodes occurred under basal conditions. Using an atrial-specific Pitx2 conditional transgenic mouse line, Chinchilla et al.<sup>7</sup> demonstrated abnormal ECGs at rest as well as impaired SCN5A ( $I_{Na}$ ), KCNJ2 ( $I_{K1}$ ) and KCNJ12 ( $I_{K1}$ ) expression and function. These observations were subsequently corroborated by Tao et al.<sup>56</sup> using a model of conditional Pitx2 expression in adult mice. Additional evidence was found for a role for Pitx2 in calcium homeostasis.<sup>8,57–60</sup> These data therefore suggest that an embryonic impairment of Pitx2 might predispose to atrial arrhythmias while an adult deficiency will be already causative of AF.

### 4.1 | Expression and distribution of lncRNAs

In this study, we have identified four distinct Wnt-associated lncRNAs with preferential expression in the atrial chambers (*Walaa*, *Walras*, *Wallrd* and *Walrad*), three of them confined to the embryonic stages (*Walaa*, *Walras* and *Wallrd*), and a fourth lncRNA that is also preferentially expressed in the adult right atrium (*Walrad*). Expression of these lncRNAs is widely distributed along several other tissues such as the liver, brain, lungs and

gastrointestinal tract. Curiously they display discordant expression profiles as compared to Wnt8 and Wnt11, during development and adulthood, suggesting a lack of regulatory influence. Importantly, three of them (*Walras*, *Wallrd* and *Walce*) are conserved in humans. *Walras* display variable degree of homology with three distinct lncRNAs adjacent to the human *WNT11* locus, being the most likely homologous one AP002340.1 lncRNAs since it displays 43% similarity and is roughly similar in size (238 nt vs 285 nt), while AP000785.1 and LINC02761 display lower similarity (25% and 31%, respectively) and are larger in size (613 nt and 388 nt, respectively). Mouse *Walrrd* presents three distinct isoform, each of them displaying homologue similarity to AC13382.1 (33%), AC13382.2 (45%) and AC1041116.1 (44%), while *Walce* displayed 35% similarity to Wnt11\_03 lncRNAs. Such findings are in line with previous results of the modest similarity of lncRNAs between distinct species.

lncRNAs are found in the nucleus and cytoplasm, primarily functioning as transcriptional or post-transcriptional modulators,<sup>61–64</sup> respectively. Our analyses demonstrate that most lncRNAs studied display dual nuclear and cytoplasmic localization i.e., *Walras*, *Walce*, *Wallrd* and *Playrr*. Importantly, both temporal and spatial differences in the nuclear vs cytoplasmic localization was observed for several of these lncRNAs, with *Walrad* being primarily nuclear in the embryonic and neonatal right and left atrial chambers but not in the ventricles, and *Walas* displaying a prominent nuclear localization in the embryonic right atrium but similarly distributed in both atrial chambers at the neonatal stage. These data underscore the highly dynamic temporal and spatial distribution of these lncRNAs during cardiogenesis and support the notion that they can exert distinct transcriptional and post-transcriptional functions.

### 4.2 | Modulation of lncRNAs

Subsequently experiments revealed that Pitx2 enhanced the expression of *Walaa* and *Walce*, while it significantly decreased the expression of *Wallrd*, supporting a role for these lncRNAs in a Pitx2-regulated processes. Analyses in an atrium-specific Pitx2 conditional transgenic mice further supported a regulatory role of Pitx2 in raising the levels of *Walaa* and *Wallrd*. Importantly, such upregulation is also observed for human *WALLRD* (AC1040116.1) in AF patients. Moreover, *WALLRAS* (AP002340.1) is downregulated in AF patients, further supporting a plausible role for these lncRNAs in Pitx2-induced AF. Surprisingly, divergent results are observed for *Wallrd* in atrium-specific Pitx2 conditional transgenic mice. It is possible that additional regulatory

mechanisms are driven by Pitx2 in non-cardiomyocyte cells. Additional experiments will be required to reconcile these findings.

More recently, GWAS have identified additional genes linked to AF pathophysiology, such as *KCNN3*, *ZFHX3*, *IL6R*, *CAV1*, *HCN4*, *SYNE2*, *SYNPOL2*, *PRRX1*, and *WTN8A*, among others.<sup>1,65–68</sup> To date more than 90 genes have been associated to AF by GWAS analyses.<sup>2</sup> Strategies to increase and reduce Pitx2, Lozano-Velasco et al.<sup>8</sup> demonstrated that Pitx2 can drive expression of *Wnt8a*, but not *Zfhx3*. Interestingly, impaired *Wnt8a* expression is only reported in Pitx2 loss-of-function models with abnormal electrophysiological parameters at rest, supporting the notion that Wnt signaling is essential for the AF susceptibility vs triggering capacity. In this context it is important to highlight that risk variants associated with increased PR interval, a condition frequently associated to AF, have been identified at the *WNT11* locus, neighboring *WALRAS* conserved human homologues (AP002340.1, AP000785.1 and LINC02761 lncRNAs).

In this study we therefore analyzed if *Wnt8* and *Wnt11* could modulate lncRNA expression as they exert synergistic and complementary regulatory mechanisms in the Pitx2>Wnt>microRNA signaling pathway as previously reported by Lozano-Velasco et al.<sup>8,9</sup> Our data demonstrate that *Wnt8* vs *Wnt11* overexpression modulate *Walrad*, *Walras* and *Walce* expression in a complementary manner. Therefore, expression of *Walrad* and *Walce* is regulated by both Pitx2 and Wnt whereas *Walras* is exclusively regulated by Wnt signaling. Thus, these data reinforce the notion of a plausible role for these lncRNAs in Pitx2>Wnt signaling and thus in atrial arrhythmias.

Different studies have reported that Pitx2-regulated microRNAs are involved in AF pathophysiology. Chinchilla et al.<sup>7</sup> demonstrated abnormal regulation of *Kcnj2* and *Kcnj12* by miR-1, leading to impaired resting membrane potential configuration in Pitx2 loss-of-function mice. Lozano-Velasco et al.<sup>8</sup> identified several microRNAs regulated by Pitx2 that were previously linked to AF in humans. In this context, miR-1, miR-133, miR-21, miR-26, miR-29 and miR-106b have previously been associated with the regulation of calcium (*CACNA1C*, *RYR2*), sodium (*SCN5A*), potassium (*KCNJ2*, *KCNE1*, *KCNB2*), cation (*HCN4*) channel subunits, respectively (revised in Ref. [11]). Importantly, microRNA regulation by Pitx2 is exerted by a balanced interplay between *Wnt8* and *Wnt11* expression.<sup>8</sup> Therefore, in the present study we tested if overexpression of Pitx2-regulated microRNAs influenced the expression of lncRNAs. Our data indicate that that microRNA overexpression can indeed modulate lncRNAs. In particular, miR-1 overexpression upregulated *Walaa* and *Wallrd*, but not *Walras*. In addition, miR-29 overexpression also significantly increased *Walaa*, while

miR-133 significantly decreased *Walaa* and *Walras*. These data reveal that the expression of *Walaa* and *Wallrd* is modulated by Pitx2 and Wnt signalling, as well as by key pro-arrhythmogenic microRNAs. Importantly, such modulatory actions seems to be indirect, as several transcription factors potentially involved in *Walaa*, *Walras* and *Playrr* regulation are distinctly impaired by miR-133 and miR-29 overexpression. Together, these data support a plausible role for these novel lncRNAs in atrial arrhythmias.

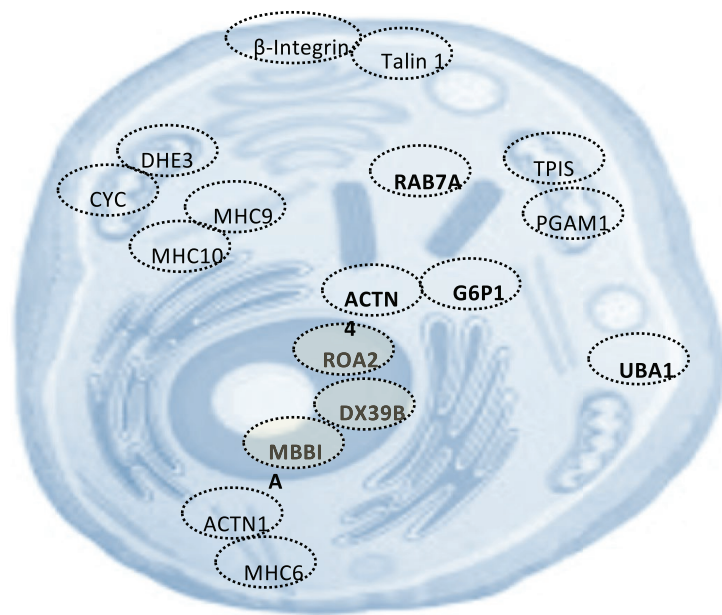
There is wide demonstration that hypertension (HTN), hyperthyroidism (HTD), diabetes and obesity promote AF onset, respectively.<sup>69–71</sup> In addition, AF occurrence can be also increased in presence of hypertrophic cardiomyopathy and valvular heart diseases.<sup>70,72,73</sup> Importantly, Pitx2 is upregulated in cardiac hypertrophy<sup>74</sup> as well as in heart failure.<sup>10</sup> We have recently provided evidence on the modulatory role of upstream pathways modulating Pitx2 in the setting of AF. HTD but not HTN leads to impaired Pitx2>Wnt>microRNA signaling causing thus abnormal ion channel expression. We herein tested whether AngII and NE treatment modulate lncRNA expression. Our data demonstrate that all lncRNAs analyzed are upregulated upon AngII and NE administration, supporting a plausible role of these lncRNAs in atrial arrhythmias as well as in cardiac hypertrophy.

In addition, we also analyzed if thyroid hormone influenced their expression. Surprisingly, thyroid hormone distinctly modulated lncRNA expression as compared to AngII/NE administration. Thus, *Walaa* was significantly downregulated after T3 administration as well as *Wallrd* after both T3 and T4 administration, respectively. On the other hand, *Walras* was significantly upregulated after both T3 and T4 administration, respectively. These data further strengthen a role for these lncRNAs in atrial arrhythmias as they display differential modulation by AngII/NE vs T3/T4 administration.

### 4.3 | Functional roles of lncRNAs

In order to start understanding the functional roles of these lncRNAs in cardiac development, pulldown assays for the lncRNA *Walras* were performed in HL1 atrial cardiomyocytes. A total of 40 proteins were identified that significantly interacted with *Walras*. Most of these proteins are cytoplasmic (>40%), suggesting a prominent extranuclear role for *Walras* (Figure 8). Two major sets of cytoplasmic proteins were found, myosin proteins (MHY6, MHY9 and MHY10) and cytoskeletal proteins (*RAB1A*, *RAB2A*, *RAB7A*, *ACTN1*, *ACTN4* and *TLN1*). Importantly, we validated a direct protein-*Walras* interaction for *ACTN4*. Point mutations in *MHY6* have been associated to cardiac hypertrophy, dilated cardiomyopathy, AF and congenital

## Walras lncRNA interacting proteins



### Cytoskeleton and membrane cell proteins

- MHC10
- MHC9
- MHC6
- $\beta$ -Integrine
- Talin 1
- ACTN1

### Cytoplasm related proteins

- G6P1
- ACTN4
- RAB7A
- UBA1

### Nuclear related proteins

- ROA2
- DX39B
- MBBIA

### Mitochondria proteins

- TPIS
- PGAM1
- DHE3
- CYC

**FIGURE 9** Schematic representation of the most prominent *Walras*-interacting proteins as identified by pulldown assays and mass spectrometry identification. Observe that *Walras* interacts with distinct cytoskeletal and cytoplasmic proteins as well as nuclear proteins mitochondrial proteins

heart diseases.<sup>75–79</sup> In addition, SNV in the proximity of *MHY6* have been associated with AF and impaired heart rate.<sup>45</sup> Experiments in mice further support the functional role of *MHY6* in cardiac pathophysiology.<sup>80</sup> *RAB7A* has been implicated in controlling  $\beta$ -adrenergic receptor endosome recycling<sup>81</sup> and impaired  $\beta$ -adrenergic stimulation is frequently associated to AF. Abnormal expression of *ACTN1* and *TLN1* leads to dilated cardiomyopathy.<sup>82–84</sup> In particular, *TLN1* knock-out display decreased beta1-integrin expression (another *Walras* interacting protein), costameric instability and cardiac hypertrophy.<sup>84</sup> Thus, it is plausible that the interaction of *Walras* with *TLN1* might contribute to stabilization of cytoskeletal proteins such as *ACTN1*, *ACTN4* and *MHY9* and *MHY10*, via *ITG1* phosphorylation,<sup>83,84</sup> a process that might be impaired in cardiac hypertrophy. In this context, we provided evidence that impairing *Walras* expression leads to decreased expression of *ACTN1*, *ACTN4* and *MHY9* in HL1 atrial cardiomyocytes. Importantly, two additional cytoplasmic *Walras*-interacting proteins are also impaired in cardiac hypertrophy, *UBA1* and *PPIA*.<sup>85–87</sup> Collectively, these lines of evidence support the idea that impairment of *Walras* might also lead to cardiac arrhythmias and/or hypertrophy by deregulating several interacting proteins (Figure 9).

*Walras* also showed affinity for nuclear proteins *ROA2*, *ROA1*, *DXC39B* and *MBBIA*, supporting a nuclear function for *Walras*. It is important to note that we found similar subcellular distribution patterns for *Walras* in other tissues analyzed, except in the embryonic right atrium and ventricles. At present, the functional roles of these interacting proteins are poorly understood. Surprisingly, *Walras* also interacts with a large array of mitochondrial proteins (*KAD2*, *PGAM1*, *DHE3*, *CPT2*, *IVD*, *CYC*, and *SDHB*) and endoplasmic reticulum proteins (*HYEP*, *NB5R3*, *RTN-4*, *CALU*, *ETFD*, and *TXDN5*). While the nature and functional consequences of such interactions remain to be explored, it is important to highlight the fact that impaired expression of *SDHD*, *CPT2*, *RTN4*, *ETFD*, and *CATD* has also been associated to hypertrophic and/or dilated cardiomyopathy,<sup>88–91</sup> reinforcing the notion that *Walras* might play a role in cardiac hypertrophy.

In summary, we have identified five novel lncRNAs that are differentially expressed in the developing and adult heart. Three of them displayed atrial expression during embryogenesis and a fourth one is expressed in the right atrium in adulthood. Signaling through *Pitx2*>*Wnt*>*miRNAs* modulates the expression of these lncRNAs. In addition, pro-hypertrophic and pro-arrhythmogenic pathways such

as those induced by AngII/NE and thyroid hormone administration distinctly regulated the expression of these lncRNAs. Pulldown and loss-of-function assays revealed that *Walras* interacts primarily with cytoplasmic proteins that, if impaired, are associated with cardiac arrhythmias and hypertrophy. Overall, these data suggest that role of these lncRNAs might play a role in cardiac arrhythmogenesis and hypertrophy.

## DISCLOSURES

The authors declare no conflicts of interest.

## AUTHOR CONTRIBUTIONS

Diego Franco, Amelia E. Aránega, Myriam Gorospe, Leif Hove-Madsen designed research; Carlos García-Padilla, Jorge N. Domínguez, Valeria Lodde, Rachel Munk, Kotb Abdelmohsen performed research; Carlos García-Padilla, Jorge N. Domínguez, Valeria Lodde, Rachel Munk, Kotb Abdelmohsen analyzed data; Veronica Jiménez-Sábado, Antonino Ginel contributed with clinical data; Diego Franco wrote the draft paper; Carlos García-Padilla, Myriam Gorospe, Leif Hove-Madsen and Diego Franco edited final manuscript.

## ORCID

Diego Franco  <https://orcid.org/0000-0002-5669-7164>

## REFERENCES

- Gudbjartsson DF, Arnar DO, Helgadóttir A, et al. Variants conferring risk of atrial fibrillation on chromosome 4q25. *Nature*. 2007;448:353-357.
- Roselli C, Chaffin MD, Weng LC, et al. Multi-ethnic genome-wide association study for atrial fibrillation. *Nat Genet*. 2018;50(9):1225-1233.
- Aguirre LA, Alonso ME, Badía-Careaga C, et al. Long-range regulatory interactions at the 4q25 atrial fibrillation risk locus involve PITX2c and ENPEP. *BMC Biol*. 2015;13:26.
- Zhang M, Hill MC, Kadow ZA, et al. Long-range *Pitx2c* enhancer-promoter interactions prevent predisposition to atrial fibrillation. *Proc Natl Acad Sci U S A*. 2019;116(45):22692-22698.
- Wang J, Klysis E, Sood S, Johnson RL, Wehrens XH, Martin JF. *Pitx2* prevents susceptibility to atrial arrhythmias by inhibiting left-sided pacemaker specification. *Proc Natl Acad Sci U S A*. 2010;107(21):9753-9758.
- Kirchhof P, Kahr PC, Kaese S, et al. PITX2c is expressed in the adult left atrium, and reducing PITX2c expression promotes atrial fibrillation inducibility and complex changes in gene expression. *Circ Cardiovasc Genet*. 2011;4:123-133.
- Chinchilla A, Daimi H, Lozano-Velasco E, et al. *Pitx2* insufficiency leads to atrial electrical and structural remodeling linked to arrhythmogenesis. *Circ Cardiovasc Genet*. 2011;4(3):269-279.
- Lozano-Velasco E, Hernández-Torres F, Daimi H, et al. *Pitx2* impairs calcium handling in a dose-dependent manner by modulating WNT signalling. *Cardiovasc Res*. 2016;109(1):55-66.
- Lozano-Velasco E, Wangenstein R, Quesada A, et al. Hyperthyroidism, but not hypertension, impairs *Pitx2* expression leading to WNT-microRNA-ion channel remodeling. *PLoS One*. 2017;12(12):e0188473.
- Torrado M, Franco D, Hernández-Torres F, et al. PITX2c is reactivated in the failing myocardium and stimulates *myf5* expression in cultured cardiomyocytes. *PLoS One*. 2014;9(3):e90561.
- Lozano-Velasco E, Garcia-Padilla C, Aránega AE, Franco D. Genetics of atrial fibrillation: in search of novel therapeutic targets. *Cardiovasc Hematol Disord Drug Targets*. 2019;19(3):183-194.
- Wapinski O, Chang HY. Long noncoding RNAs and human disease. *Trends Cell Biol*. 2011;21(6):354-361.
- Engreitz JM, Ollikainen N, Guttman M. Long non-coding RNAs: spatial amplifiers that control nuclear structure and gene expression. *Nat Rev Mol Cell Biol*. 2016;17(12):756-770.
- Gloss BS, Dinger ME. The specificity of long noncoding RNA expression. *Biochim Biophys Acta*. 2016;1859(1):16-22.
- Bär C, Chatterjee S, Thum T. Long noncoding RNAs in cardiovascular pathology, diagnosis, and therapy. *Circulation*. 2016;134(19):1484-1499.
- Chen L. Linking long noncoding RNA localization and function. *Trends Biochem Sci*. 2016;41(9):761-772.
- Ounzain S, Micheletti R, Arnan C, et al. CARMEN, a human super enhancer-associated long noncoding RNA controlling cardiac specification, differentiation and homeostasis. *J Mol Cell Cardiol*. 2015;89:98-112.
- Boucher JM, Peterson SM, Urs S, et al. The miR-143/145 cluster is a novel transcriptional target of Jagged-1/Notch signaling in vascular smooth muscle cells. *J Biol Chem*. 2011;286(32):28312-28321.
- Klattenhoff C, Scheuermann J, Surface L, et al. Braveheart, a long noncoding RNA required for cardiovascular lineage commitment. *Cell*. 2013;152(3):570-583.
- Mahlapuu M, Ormestad M, Enerback S, et al. The forkhead transcription factor *Foxf1* is required for differentiation of extra-embryonic and lateral plate mesoderm. *Development*. 2001;128(2):155-166.
- Grote P, Wittler L, Hendrix D, et al. The tissue-specific lncRNA *Fendrr* is an essential regulator of heart and body wall development in the mouse. *Dev Cell*. 2013;24(2):206-214.
- Garcia-Padilla C, Dominguez JN, Aránega A, Franco D. Differential chamber-specific expression and regulation of long non coding RNAs during cardiac development. *Biochim Biophys Acta Gene Regul Mech*. 2019;1862(10):194435.
- Ruan Z, Sun X, Sheng H, Zhu L. Long non-coding RNA expression profile in atrial fibrillation. *Int J Clin Exp Pathol*. 2015;8(7):8402-8410.
- Su Y, Li L, Zhao S, Yue Y, Yang S. The long noncoding RNA expression profiles of paroxysmal atrial fibrillation identified by microarray analysis. *Gene*. 2018;642:125-134.
- Mei B, Liu H, Yang S, et al. Long non-coding RNA expression profile in permanent atrial fibrillation patients with rheumatic heart disease. *Eur Rev Med Pharmacol Sci*. 2018;22(20):6940-6947.
- Qian C, Li H, Chang D, Wei B, Wang Y. Identification of functional lncRNAs in atrial fibrillation by integrative analysis of the lncRNA-mRNA network based on competing endogenous RNAs hypothesis. *J Cell Physiol*. 2019;234(7):11620-11630.
- Gore-Panter SR, Hsu J, Barnard J, et al. PANCR, the *Pitx2* adjacent noncoding RNA, is expressed in human left atria and regulates PITX2c expression. *Circ Arrhythm Electrophysiol*. 2016;9(1):e003197.

28. Gage PJ, Suh H, Camper SA. Dosage requirement of *Pitx2* for development of multiple organs. *Development*. 1999;126:4643-4651.
29. de Lange FJ, Moorman AF, Christoffels VM. Atrial cardiomyocyte-specific expression of Cre recombinase driven by an *Nppa* gene fragment. *Genesis*. 2003;37:1-4.
30. Livak KJ, Schmittgen TD. Analysis of relative gene expression data using real-time quantitative PCR and the 2(-Delta Delta C(T)) Method. *Methods*. 2001;25:402-408.
31. Daimi H, Lozano-Velasco E, Haj Khelil A, et al. Regulation of *SCN5A* by microRNAs: miR-219 modulates *SCN5A* transcript expression and the effects of flecainide intoxication in mice. *Heart Rhythm*. 2015;12:1333-1342.
32. Wang YG, Dedkova EN, Fiening JP, Ojamaa K, Blatter LA, Lipsius SL. Acute exposure to thyroid hormone increases  $\text{Na}^+$  current and intracellular  $\text{Ca}^{2+}$  in cat atrial myocytes. *J Physiol*. 2003;546(Pt 2):491-499.
33. Lunde IG, Kvaløy H, Austbø B, Christensen G, Carlson CR. Angiotensin II and norepinephrine activate specific calcineurin-dependent NFAT transcription factor isoforms in cardiomyocytes. *J Appl Physiol*. 2011;111(5):1278-1289.
34. Panda AC, Martindale JL, Gorospe M. Affinity pulldown of biotinylated RNA for detection of protein-RNA complexes. *Bio Protoc*. 2016;6(24):e2062.
35. Villegas VE, Zaphiropoulos PG. Neighboring gene regulation by antisense long non-coding RNAs. *Int J Mol Sci*. 2015;16(2):3251-3266.
36. Dempsey J, Zhang A, Cui JY. Coordinate regulation of long non-coding RNAs and protein-coding genes in germ-free mice. *BMC Genom*. 2018;19(1):834.
37. Hori Y, Tanimoto Y, Takahashi S, Furukawa T, Koshiba-Takeuchi K, Takeuchi JK. Important cardiac transcription factor genes are accompanied by bidirectional long non-coding RNAs. *BMC Genom*. 2018;19(1):967.
38. Hitachi K, Nakatani M, Takasaki A, et al. Myogenin promoter-associated lncRNA *Myoparr* is essential for myogenic differentiation. *EMBO Rep*. 2019;20(3):e47468.
39. Welsh IC, Kwak H, Chen FL, et al. Chromatin architecture of the *Pitx2* locus requires CTCF- and *Pitx2*-dependent asymmetry that mirrors embryonic gut laterality. *Cell Rep*. 2015;13(2):337-349.
40. Higa S, Maesato A, Ishigaki S, Suenari K, Chen YJ, Chen SA. Diabetes and endocrine disorders (hyperthyroidism/hypothyroidism) as risk factors for atrial fibrillation. *Card Electrophysiol Clin*. 2021;13(1):63-75.
41. Tribulova N, Kurahara LH, Hlivak P, Hirano K, Szeiffova BB. Pro-arrhythmic signaling of thyroid hormones and its relevance in subclinical hyperthyroidism. *Int J Mol Sci*. 2020;21(8):2844.
42. Barreto-Chaves ML, Senger N, Fevereiro M, Parletta AC, Takano A. Impact of hyperthyroidism on cardiac hypertrophy. *Endocr Connect*. 2020;9(3):R59-R69.
43. Prisant LM, Gujral JS, Mulloy AL. Hyperthyroidism: a secondary cause of isolated systolic hypertension. *J Clin Hypertens (Greenwich)*. 2006;8(8):596-599.
44. Dörr M, Völzke H. Cardiovascular morbidity and mortality in thyroid dysfunction. *Minerva Endocrinol*. 2005;30(4):199-216.
45. Holm H, Gudbjartsson DF, Sulem P, et al. A rare variant in *MYH6* is associated with high risk of sick sinus syndrome. *Nat Genet*. 2011;43(4):316-320.
46. Wolf CM. Hypertrophic cardiomyopathy: genetics and clinical perspectives. *Cardiovasc Diagn Ther*. 2019;9(Suppl 2):S388-S415.
47. Marian AJ, Braunwald E. Hypertrophic cardiomyopathy: genetics, pathogenesis, clinical manifestations, diagnosis, and therapy. *Circ Res*. 2017;121(7):749-770.
48. McNally EM, Golbus JR, Puckelwartz MJ. Genetic mutations and mechanisms in dilated cardiomyopathy. *J Clin Invest*. 2013;123(1):19-26.
49. Veluchamy A, Ballerini L, Vitart V, et al. Novel genetic locus influencing retinal venular tortuosity is also associated with risk of coronary artery disease. *Arterioscler Thromb Vasc Biol*. 2019;39(12):2542-2552.
50. Jalife J, Kaur K. Atrial remodeling, fibrosis, and atrial fibrillation. *Trends Cardiovasc Med*. 2015;25(6):475-484. doi:10.1016/j.tcm.2014.12.015
51. Henningsen KM, Olesen MS, Haunsoe S, Svendsen JH. Association of rs2200733 at 4q25 with early onset of lone atrial fibrillation in young patients. *Scand Cardiovasc J*. 2011;45:324-326.
52. Kiliszek M, Franaszczyk M, Kozluk E, et al. Association between variants on chromosome 4q25, 16q22 and 1q21 and atrial fibrillation in the Polish population. *PLoS One*. 2011;6(7):e21790.
53. Olesen MS, Holst AG, Jabbari J, et al. Genetic loci on chromosomes 4q25, 7p31, and 12p12 are associated with onset of lone atrial fibrillation before the age of 40 years. *Can J Cardiol*. 2012;28:191-195.
54. Parvez B, Shoemaker MB, Muhammad R, et al. Common genetic polymorphism at 4q25 locus predicts atrial fibrillation recurrence after successful cardioversion. *Heart Rhythm*. 2013;10(6):849-855.
55. Mohanty S, Santangeli P, Bai R, et al. Variant rs2200733 on chromosome 4q25 confers increased risk of atrial fibrillation: evidence from a meta-analysis. *J Cardiovasc Electrophysiol*. 2013;24:155-161.
56. Tao Y, Zhang M, Li L, et al. *Pitx2*, an atrial fibrillation predisposition gene, directly regulates ion transport and intercalated disc genes. *Circ Cardiovasc Genet*. 2014;7:23-32.
57. Pérez-Hernández M, Matamoros M, Barana A, et al. *Pitx2c* increases in atrial myocytes from chronic atrial fibrillation patients enhancing IKs and decreasing I<sub>Ca,L</sub>. *Cardiovasc Res*. 2016;109(3):431-441.
58. Bai J, Gladding PA, Stiles MK, Fedorov VV, Zhao J. Ionic and cellular mechanisms underlying *TBX5/PITX2* insufficiency-induced atrial fibrillation: insights from mathematical models of human atrial cells. *Sci Rep*. 2018;8(1):15642.
59. Bai J, Lo A, Gladding PA, Stiles MK, Fedorov VV, Zhao J. In silico investigation of the mechanisms underlying atrial fibrillation due to impaired *Pitx2*. *PLoS Comput Biol*. 2020;16(2):e1007678.
60. Bai J, Zhu Y, Lo A, Lu Y, Zhao J. In silico assessment of genetic variation in *PITX2* reveals the molecular mechanisms of calcium-mediated cellular triggered activity in atrial fibrillation. *Annu Int Conf IEEE Eng Med Biol Soc*. 2020;2020:2353-2356.
61. Terreri S, Mancinelli S, Ferro M, et al. Subcellular localization of uc8+ as a prognostic biomarker in bladder cancer tissue. *Cancers (Basel)*. 2021;13(4):681.
62. Das S, Zhang E, Senapati P, et al. A novel angiotensin II-induced long noncoding RNA giver regulates oxidative stress, inflammation, and proliferation in vascular smooth muscle cells. *Circ Res*. 2018;123(12):1298-1312.

63. Cabili MN, Dunagin MC, McClanahan PD, et al. Localization and abundance analysis of human lncRNAs at single-cell and single-molecule resolution. *Genome Biol.* 2015;16(1):20.
64. Coassin SR, Orjalo AV Jr, Semaan SJ, Johansson HE. Simultaneous detection of nuclear and cytoplasmic RNA variants utilizing Stellaris® RNA fluorescence in situ hybridization in adherent cells. *Methods Mol Biol.* 2014;1211:189-199.
65. Kääb S, Darbar D, van Noord C, et al. Large scale replication and meta-analysis of variants on chromosome 4q25 associated with atrial fibrillation. *Eur Heart J.* 2009;30:813-819.
66. Schnabel RB, Kerr KF, Lubitz SA, et al.; Candidate Gene Association Resource (CARE) Atrial Fibrillation/Electrocardiography Working Group. Large-scale candidate gene analysis in whites and African Americans identifies IL6R polymorphism in relation to atrial fibrillation: the National Heart, Lung, and Blood Institute's Candidate Gene Association Resource (CARE) project. *Circ Cardiovasc Genet.* 2011;4:557-564.
67. Ellinor PT, Lunetta KL, Glazer NL, et al. Common variants in KCNN3 are associated with lone atrial fibrillation. *Nat Genet.* 2010;42:240-244.
68. Pfeufer A, van Noord C, Marcianti KD, et al. Genome-wide association study of PR interval. *Nat Genet.* 2010;42(2):153-159.
69. Zhang Q, Liu T, Ng CY, Li G. Diabetes mellitus and atrial remodeling: mechanisms and potential upstream therapies. *Cardiovasc Ther.* 2014;32:233-241.
70. Anumonwo JM, Kalifa J. Risk factors and genetics of atrial fibrillation. *Cardiol Clin.* 2014;32:485-494.
71. Goudis CA, Korantzopoulos P, Ntalas IV, Kallergis EM, Ketikoglou DG. Obesity and atrial fibrillation: a comprehensive review of the pathophysiological mechanisms and links. *J Cardiol.* 2015;66(5):361-369.
72. Yadava M, Hughey AB, Crawford TC. Postoperative atrial fibrillation: incidence, mechanisms, and clinical correlates. *Cardiol Clin.* 2014;32:627-636.
73. Kumar KR, Mandleywala SN, Link MS. Atrial and ventricular arrhythmias in hypertrophic cardiomyopathy. *Card Electrophysiol Clin.* 2015;7:173-186.
74. Su D, Jing S, Guan L, et al. Role of Nodal-PITX2C signaling pathway in glucose-induced cardiomyocyte hypertrophy. *Biochem Cell Biol.* 2014;92(3):183-190.
75. Carniel E, Taylor MR, Sinagra G, et al. Alpha-myosin heavy chain: a sarcomeric gene associated with dilated and hypertrophic phenotypes of cardiomyopathy. *Circulation.* 2005;112(1):54-59.
76. Hershberger RE, Norton N, Morales A, Li D, Siegfried JD, Gonzalez-Quintana J. Coding sequence rare variants identified in MYBPC3, MYH6, TPM1, TNNC1, and TNNI3 from 312 patients with familial or idiopathic dilated cardiomyopathy. *Circ Cardiovasc Genet.* 2010;3(2):155-161.
77. Holm H, Gudbjartsson DF, Arnar DO, et al. Several common variants modulate heart rate, PR interval and QRS duration. *Nat Genet.* 2010;42(2):117-122.
78. Granados-Riveron JT, Ghosh TK, Pope M, et al. Alpha-cardiac myosin heavy chain (MYH6) mutations affecting myofibril formation are associated with congenital heart defects. *Hum Mol Genet.* 2010;19(20):4007-4016.
79. Nielsen JB, Thorolfsdottir RB, Fritsche LG, et al. Biobank-driven genomic discovery yields new insight into atrial fibrillation biology. *Nat Genet.* 2018;50(9):1234-1239.
80. Jiang J, Wakimoto H, Seidman JG, Seidman CE. Allele-specific silencing of mutant Myh6 transcripts in mice suppresses hypertrophic cardiomyopathy. *Science.* 2013;342(6154):111-114.
81. Nooh MM, Bahouth SW. Two barcodes encoded by the type-1 PDZ and by phospho-Ser(312) regulate retromer/WASH-mediated sorting of the  $\beta(1)$ -adrenergic receptor from endosomes to the plasma membrane. *Cell Signal.* 2017;29:192-208.
82. Jia Y, Chang HC, Schipma MJ, et al. Cardiomyocyte-specific ablation of Med1 subunit of the mediator complex causes lethal dilated cardiomyopathy in mice. *PLoS One.* 2016;11(8):e0160755.
83. Manso AM, Li R, Monkley SJ, et al. Talin1 has unique expression versus talin 2 in the heart and modifies the hypertrophic response to pressure overload. *J Biol Chem.* 2013;288(6):4252-4264.
84. Manso AM, Okada H, Sakamoto FM, et al. Loss of mouse cardiomyocyte talin-1 and talin-2 leads to  $\beta$ -1 integrin reduction, costameric instability, and dilated cardiomyopathy. *Proc Natl Acad Sci U S A.* 2017;114(30):E6250-E6259.
85. Satoh K, Nigro P, Zeidan A, et al. Cyclophilin A promotes cardiac hypertrophy in apolipoprotein E-deficient mice. *Arterioscler Thromb Vasc Biol.* 2011;31(5):1116-1123.
86. Wang KC, Lim CH, McMillen IC, Duffield JA, Brooks DA, Morrison JL. Alteration of cardiac glucose metabolism in association to low birth weight: experimental evidence in lambs with left ventricular hypertrophy. *Metabolism.* 2013;62(11):1662-1672.
87. Shu Q, Lai S, Wang XM, et al. Administration of ubiquitin-activating enzyme UBA1 inhibitor PYR-41 attenuates angiotensin II-induced cardiac remodeling in mice. *Biochem Biophys Res Commun.* 2018;505(1):317-324.
88. Zhou B, Rao L, Li Y, et al. The association between dilated cardiomyopathy and RTN4 3'UTR insertion/deletion polymorphisms. *Clin Chim Acta.* 2009;400(1-2):21-24.
89. Tang Y, Mi C, Liu J, Gao F, Long J. Compromised mitochondrial remodeling in compensatory hypertrophied myocardium of spontaneously hypertensive rat. *Cardiovasc Pathol.* 2014;23(2):101-106.
90. Sasagawa S, Nishimura Y, Okabe S, et al. Downregulation of GSTK1 is a common mechanism underlying hypertrophic cardiomyopathy. *Front Pharmacol.* 2016;7:162.
91. Pereyra AS, Hasek LY, Harris KL, et al. Loss of cardiac carnitine palmitoyltransferase 2 results in rapamycin-resistant, acetylation-independent hypertrophy. *J Biol Chem.* 2017;292(45):18443-18456.

## SUPPORTING INFORMATION

Additional supporting information may be found in the online version of the article at the publisher's website.

**How to cite this article:** García-Padilla C, Domínguez JN, Lodde V, et al. Identification of atrial-enriched lncRNA *Walras* linked to cardiomyocyte cytoarchitecture and atrial fibrillation. *FASEB J.* 2022;36:e22051. doi:[10.1096/fj.202100844RR](https://doi.org/10.1096/fj.202100844RR)